Transcription factors involved in nitrogen sensing

nature COMMUNICATIONS

ARTICLE

Received 31 Mar 2015 | Accepted 9 Sep 2016 | Published 12 Oct 2016

DOI: 10.1038/ncomms13179 OPEN

NIN-like protein 8 is a master regulator of nitrate-promoted seed germination in *Arabidopsis*

Dawei Yan[1], Vanathy Easwaran[1], Vivian Chau[1], Masanori Okamoto[2,3], Matthew Ierullo[1], Mitsuhiro Kimura[1,†], Akira Endo[1,†], Ryoichi Yano[4], Asher Pasha[1,5], Yunchen Gong[1,5], Yong-Mei Bi[6], Nicolas Provart[1,5], David Guttman[1,5], Anne Krapp[7], Steven J. Rothstein[6] & Eiji Nambara[1,5]

NIN-like protein (NLP) have been shown to be involved in nitrate responses

- NLPs have been shown to directly bind to the nitrate-responsive cis-element (NRE) to induce nitrate-mediated transcription

NIN-like protein (NLP), rhizobium formation in *Lotus*

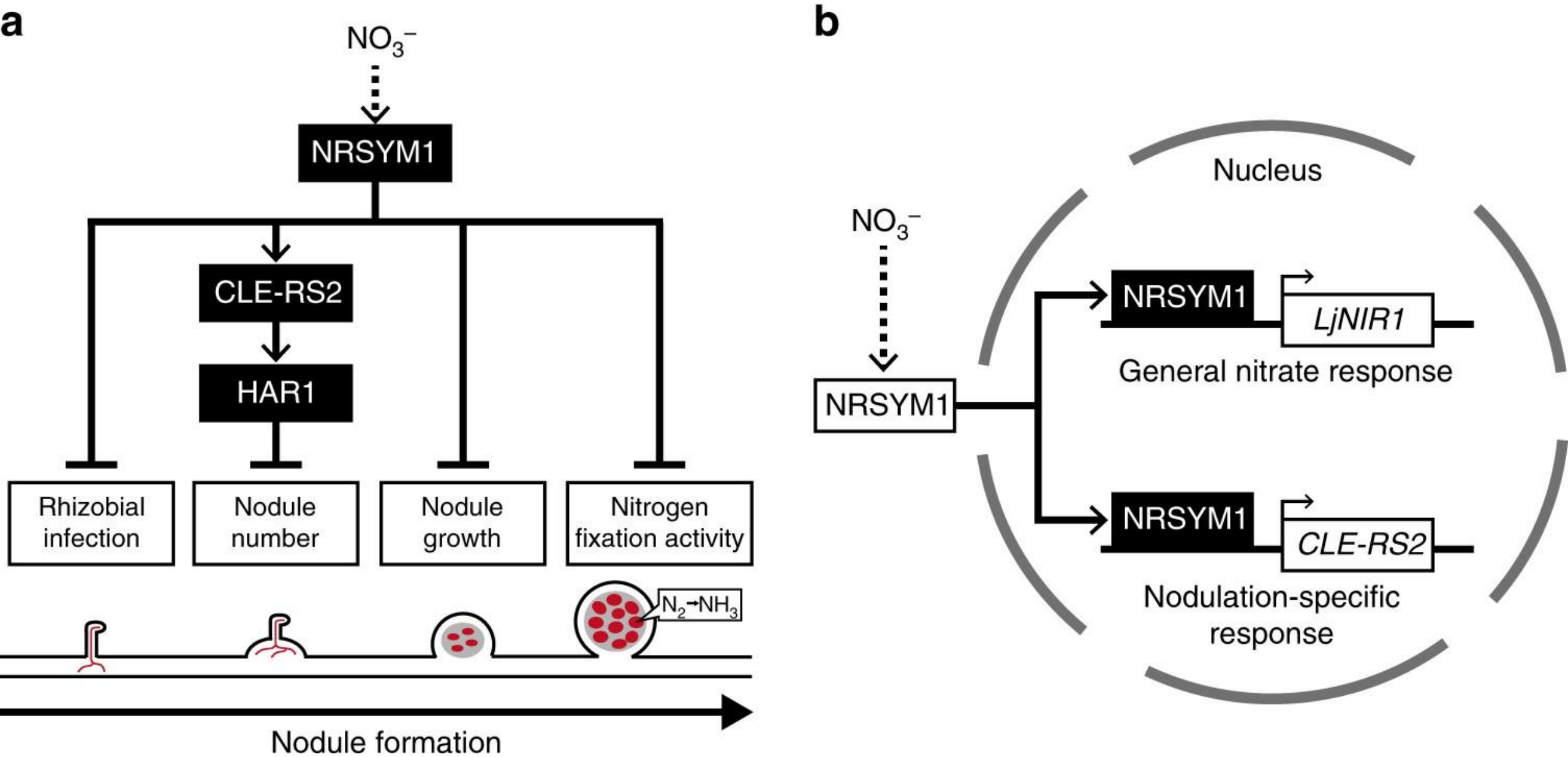
a
NO_3^-
NRSYM1
CLE-RS2
HAR1
Rhizobial infection
Nodule number
Nodule growth
Nitrogen fixation activity
$N_2 \rightarrow NH_3$
Nodule formation
b
NO_3^-
NRSYM1
Nucleus
NRSYM1
LjNIR1
General nitrate response
NRSYM1
CLE-RS2
Nodulation-specific response

Nitrate promotes seed germination in an NLP8-dependent manner.

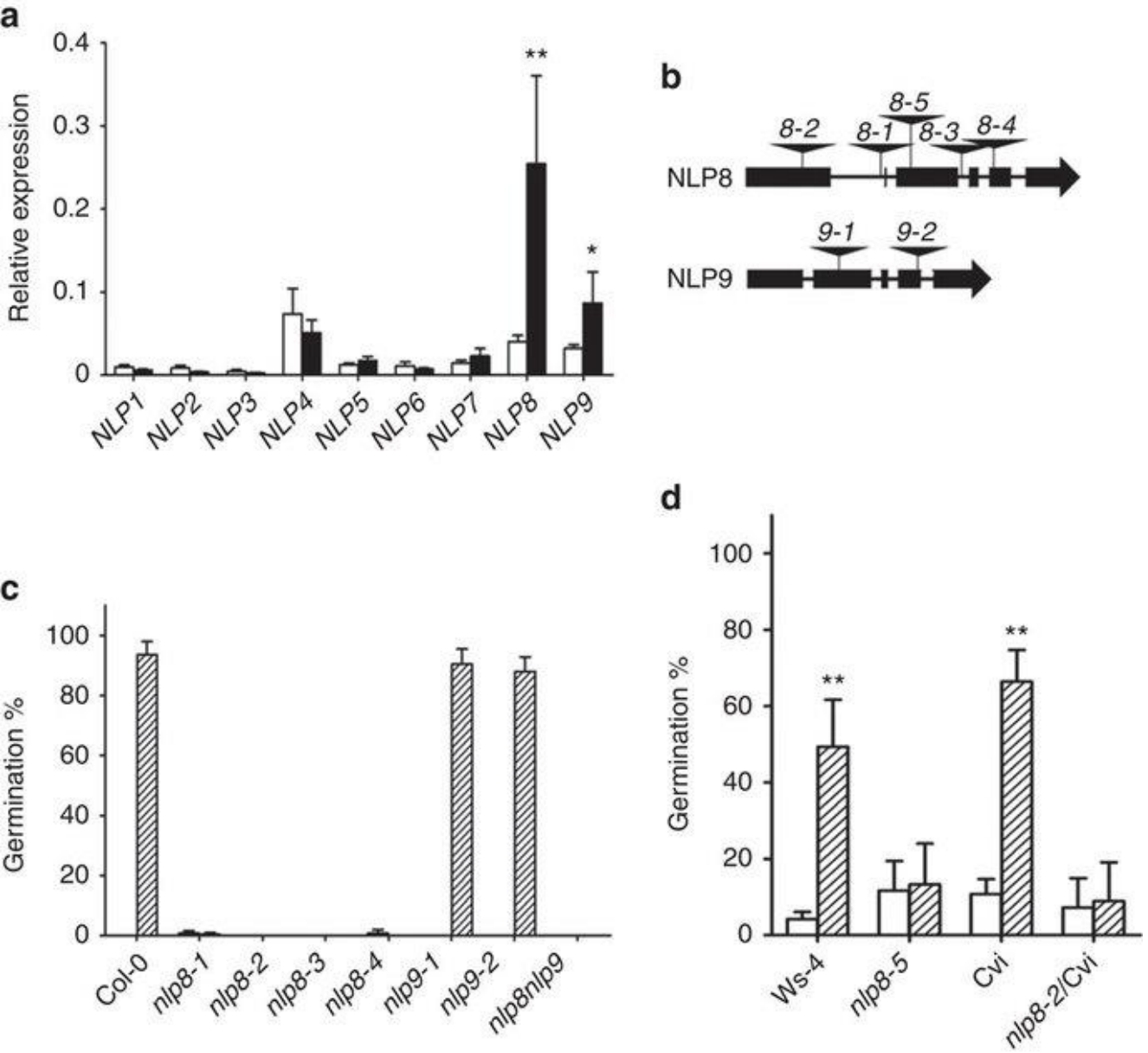

(a) Relative expression level of NLPs in dry seeds (white bar) and 6-h imbibed Col-0 seeds (black bar) from 16 °C. (b) Locations of T-DNA insertions in the *NLP8* and *NLP9*. (c) Seeds were imbibed in water with 1 mM KCl (white bar) or KNO_3 (lined bar) for 7 days. Note that all samples did not germinate in water with 1 mM KCl, thus the white bars are invisible. (d) Germination of *nlp8* mutants of Ws-4 and Cvi backgrounds in the presence of nitrate. Seeds were harvested from plants grown at 22 °C. Freshly harvested Ws-4 and *nlp8-5*, and 2-month stored Cvi and *nlp8-2*/Cvi were used for germination tests. Seeds were imbibed in water with 1 mM KCl (white bar) or KNO_3 (lined bar) for 7 days.

Insertion 9.1

Inorder to characterize this locus by PCR, in which region do you design primers:

- The insertion in mutant allele
- The WT allele

Effect of dry storage on dormancy release.

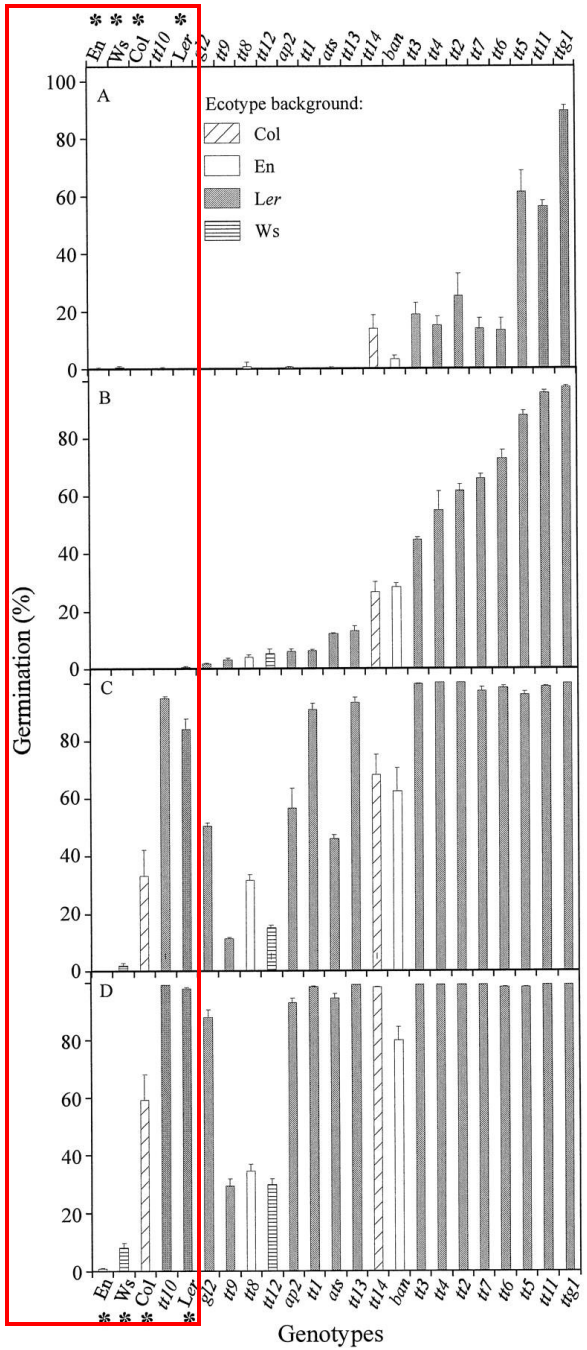

Germination was scored 2 d (A), 9 d (B), 18 d (C), and 27 d (D) after seed harvest.

Differences in germination in different ecotypes

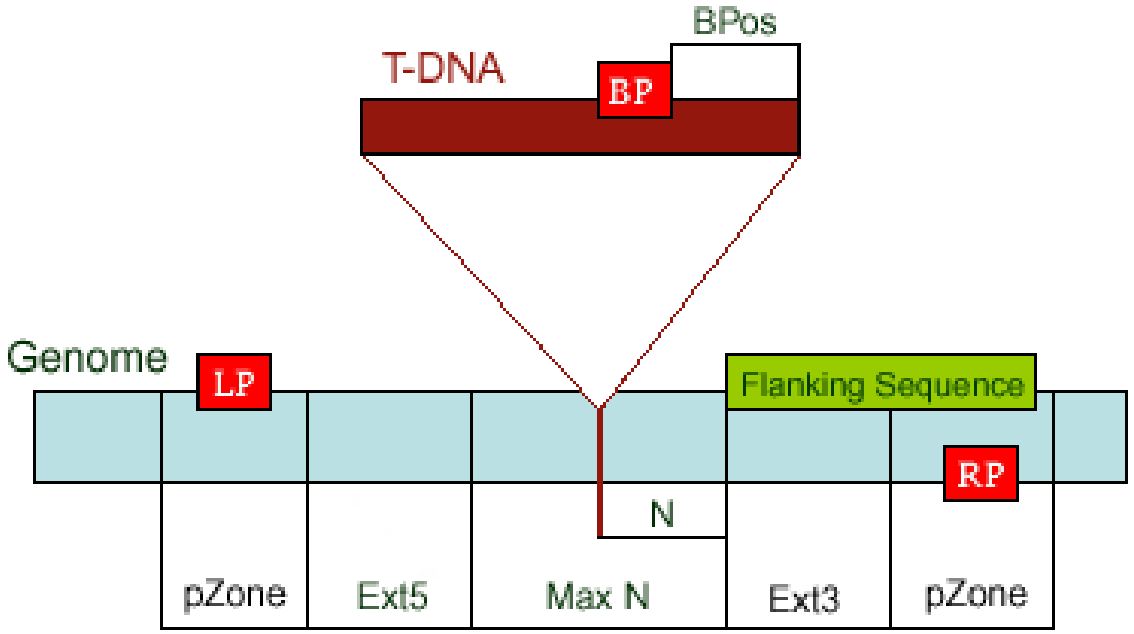
BPos
T-DNA
BP
Genome
LP
Flanking Sequence
RP
N
pZone
Ext5
Max N
Ext3
pZone

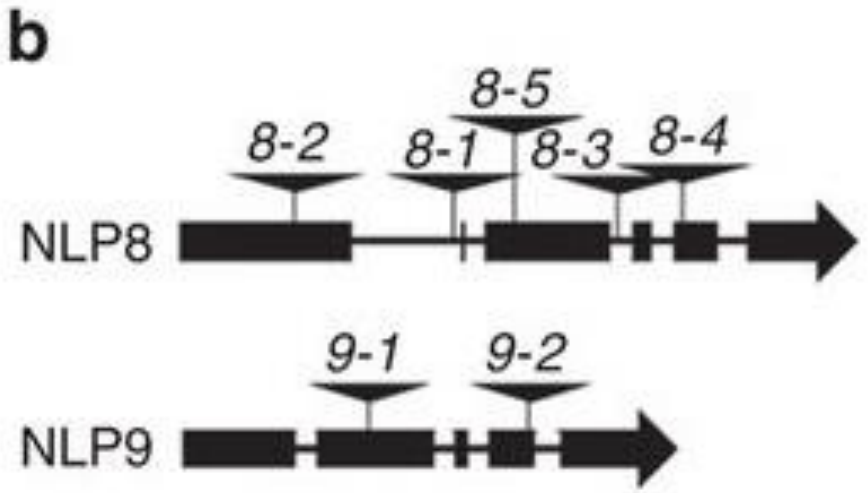
b
8-5
8-2
8-1
8-3
8-4
NLP8
9-1
9-2
NLP9

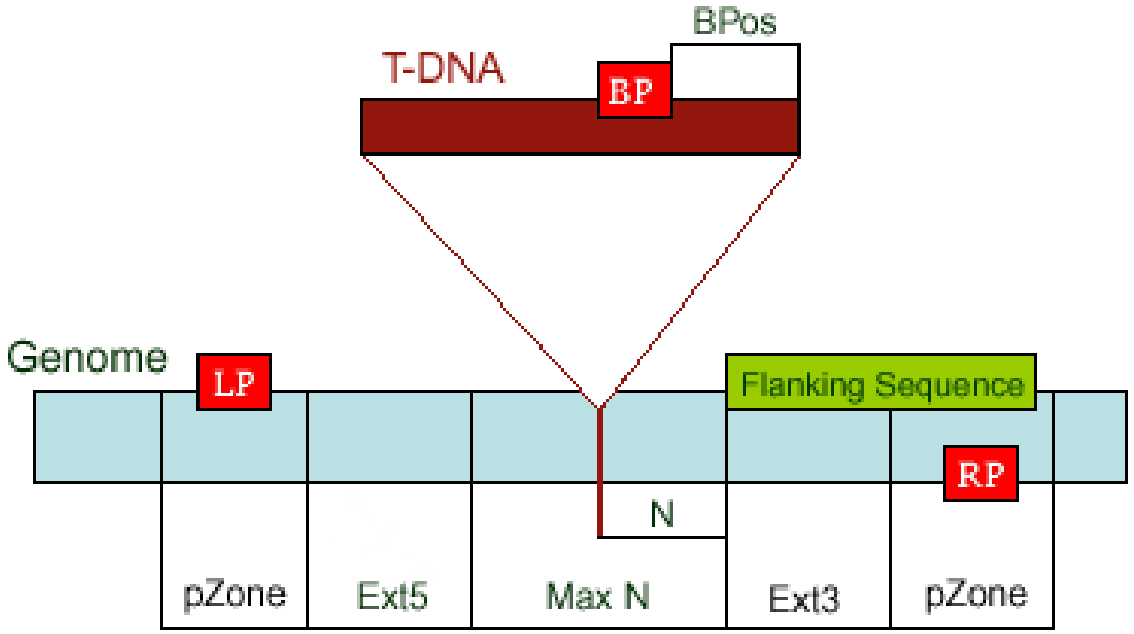
BPos
T-DNA
BP
Genome
LP
Flanking Sequence
RP
N
pZone
Ext5
Max N
Ext3
pZone


WT
HZ
HM
900
410+N
* N = 0 ~ 300

NLP8 is a master regulator for nitrate-induced gene expression during seed germination.

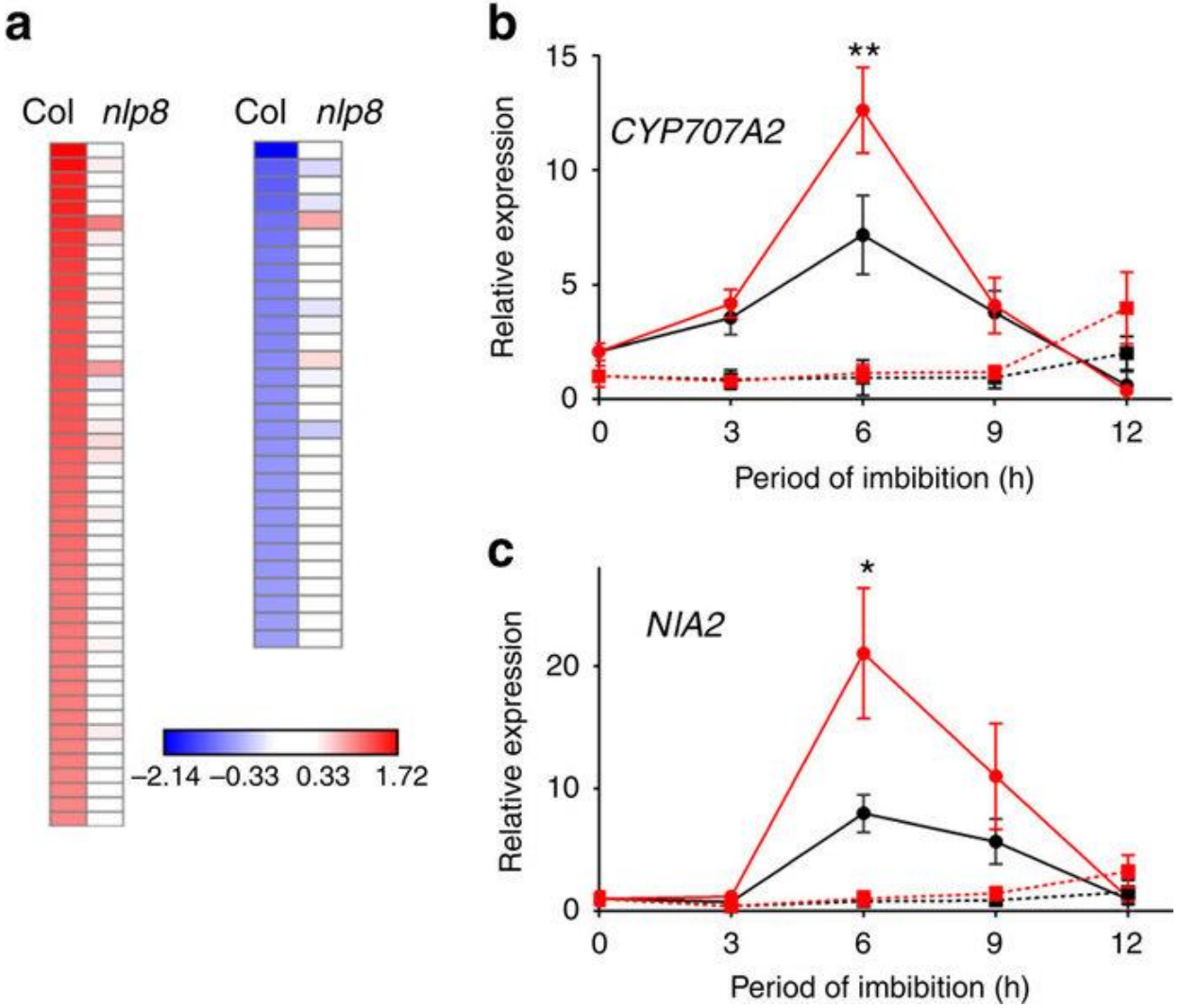

ABA CATABOLISM

Col-0 imbibed in KCl, black circle with solid line; Col-0 imbibed in KNO3, red circle with solid line; nlp8-2 imbibed in KCl, black square with dotted line; nlp8-2 imbibed in KNO3, red square with dotted line.

NITRATE REDUCTASE

Nitrate-upregulated (left) and downregulated (right) genes in 6-h imbibed seeds in Col-0 or the nlp8-2 mutant. Seeds were imbibed in water with 1mM KCl or KNO_3 for 6 h and RNA was extracted for RNA-seq.

NLP8 regulates ABA catabolism during seed germination. (a) Quantification of **ABA contents** in Col-0 and nlp8-2 seeds. Seeds were imbibed in water with 1mM KCl or KNO_3 for the indicated time periods. The ABA content was measured by liquid chromatography equipped with a mass spectrometry. (b) Germination of ABA metabolism and nlp8 mutants in the presence of nitrate.

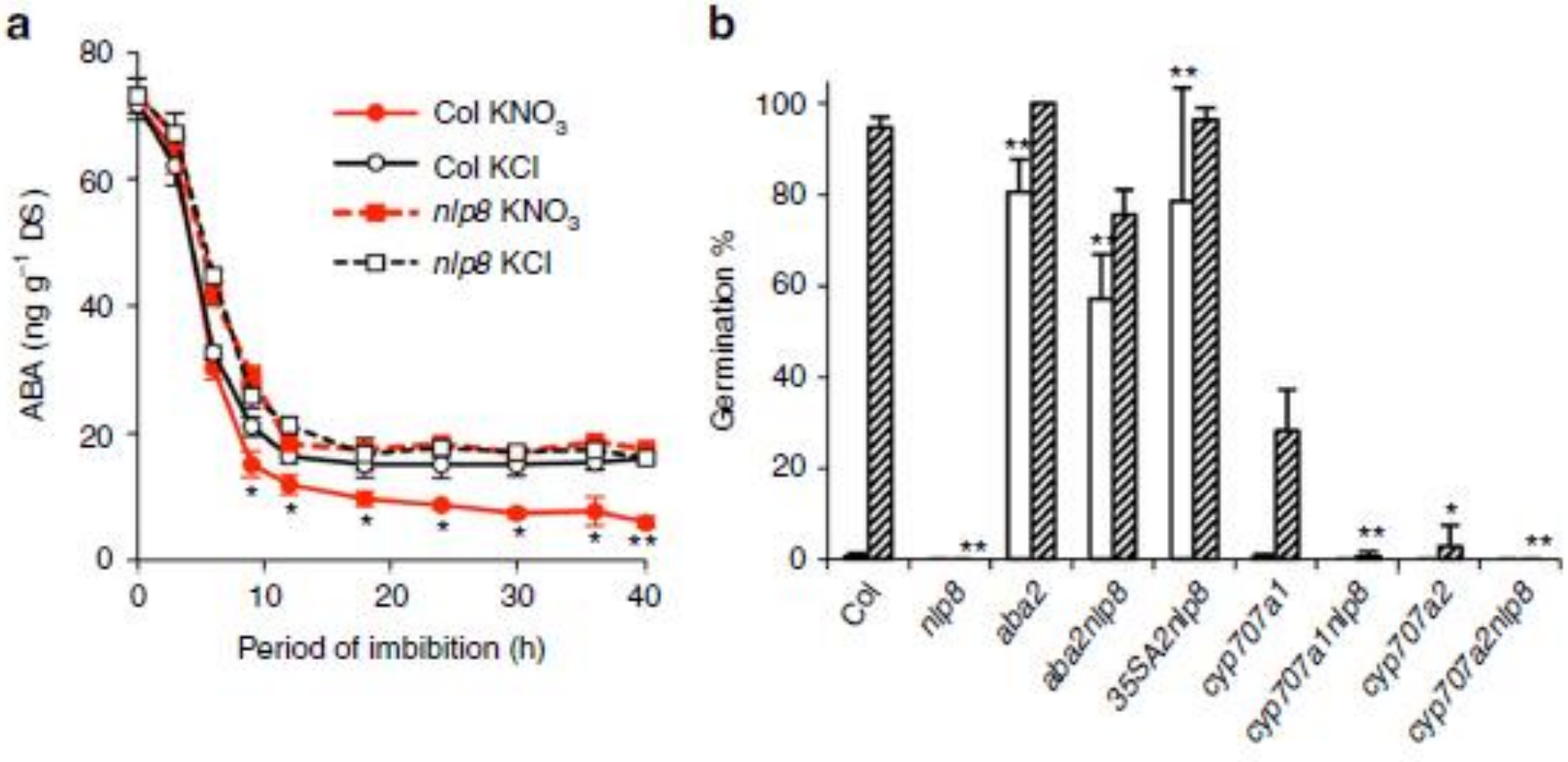

NLP8 binding motifs

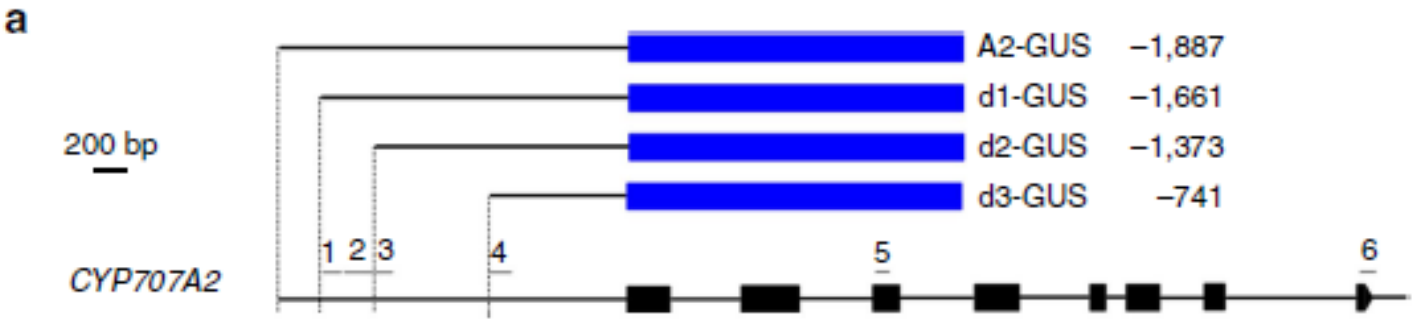

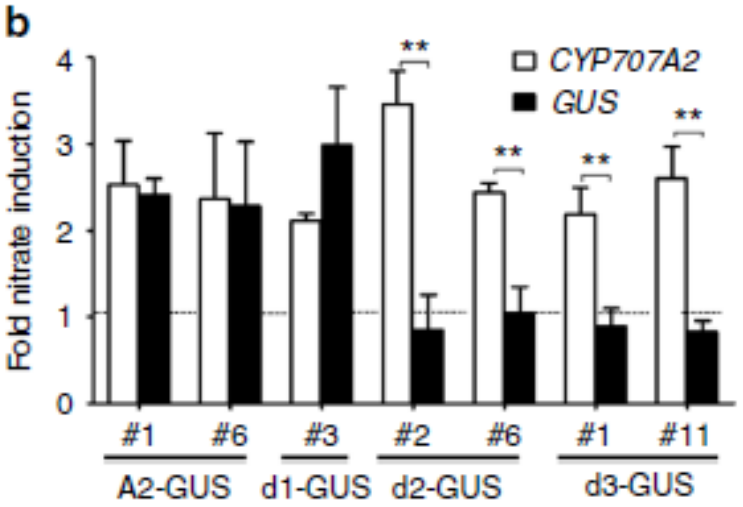

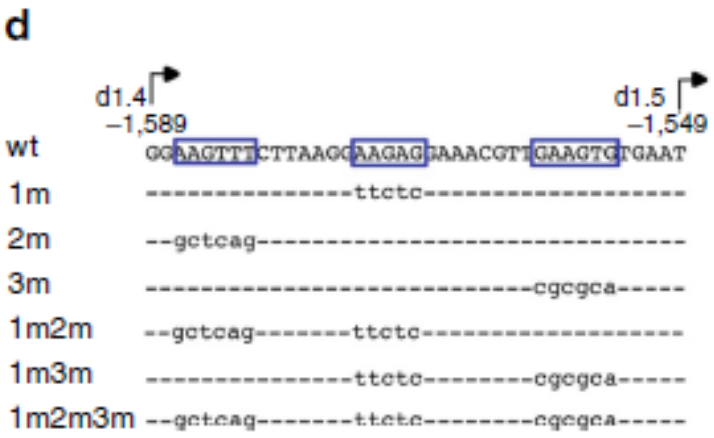

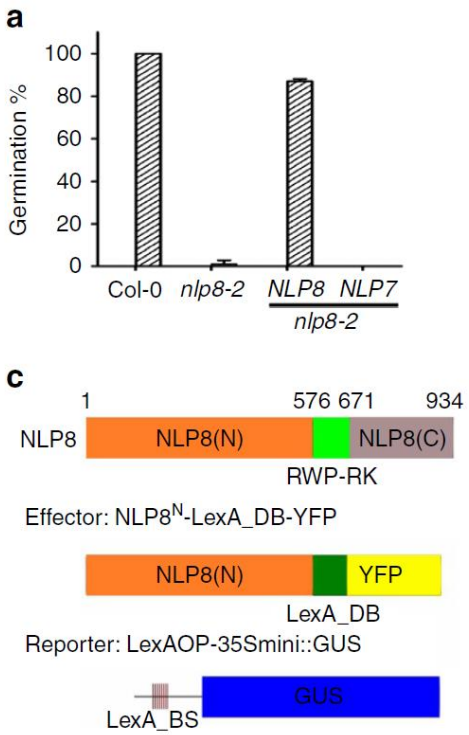

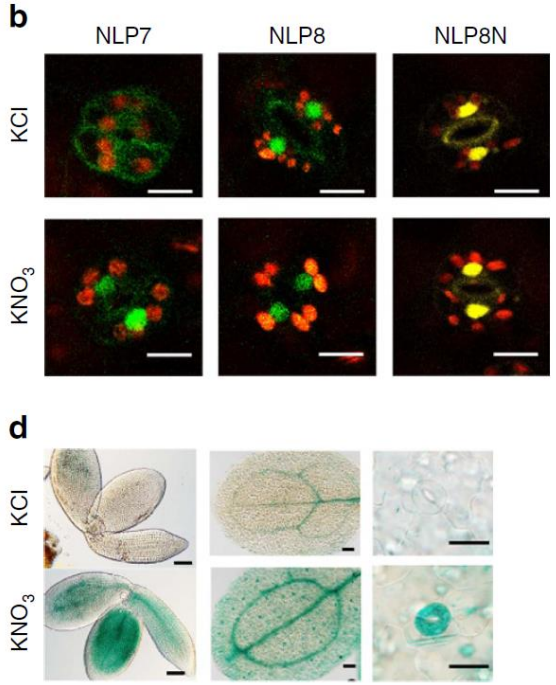

Figure 6 | Nitrate regulates NLP8 post-transcriptionally through its N-terminal region. (**a**) Complementation of *nlp8-2* by *35S::NLP8-GFP*, but not by *35S::NLP7-GFP*. Percentage of germination is shown by a mean ± s.d. ($n = 3$). (**b**) Subcellular localization of NLP8-GFP and NLP8N-LexA_DB-YFP in the stomata of KCl- or KNO_3-treated cotyledons. NLP7-GFP was used as a control for the nitrate-regulated nuclear retention. A bar indicates 10 μm. (**c**) Schematic diagram of effector construct (NLP8N-LexA_DB-YFP) harboring the N-terminal region of NLP8 (NLP8(N)), LexA DNA-binding domain (LexA_DB) and YFP, while the reporter is GUS driven by eight copies of LexA operon fused to 35S minimal promoter (LexAOP-35Smini::GUS). (**d**) GUS staining of transgenic lines harbouring both effector (NLP8N-LexA_DB-YFP) and reporter (LexAOP-35Smini::GUS). Left panel, 10 mM KCl- and KNO_3-treated 18-h-imbibed embryos; middle panel, cotyledons of 7-day-old seedlings treated with 3 mM KCl and KNO_3; guard cells at the cotyledons of 7-day-old seedlings treated with 3 mM KCl and KNO_3. From left to right, bars indicate 100, 100 and 20 μm.

A proposed schematic model for NLP8 activity in regulating nitrate-promoted seed germination.

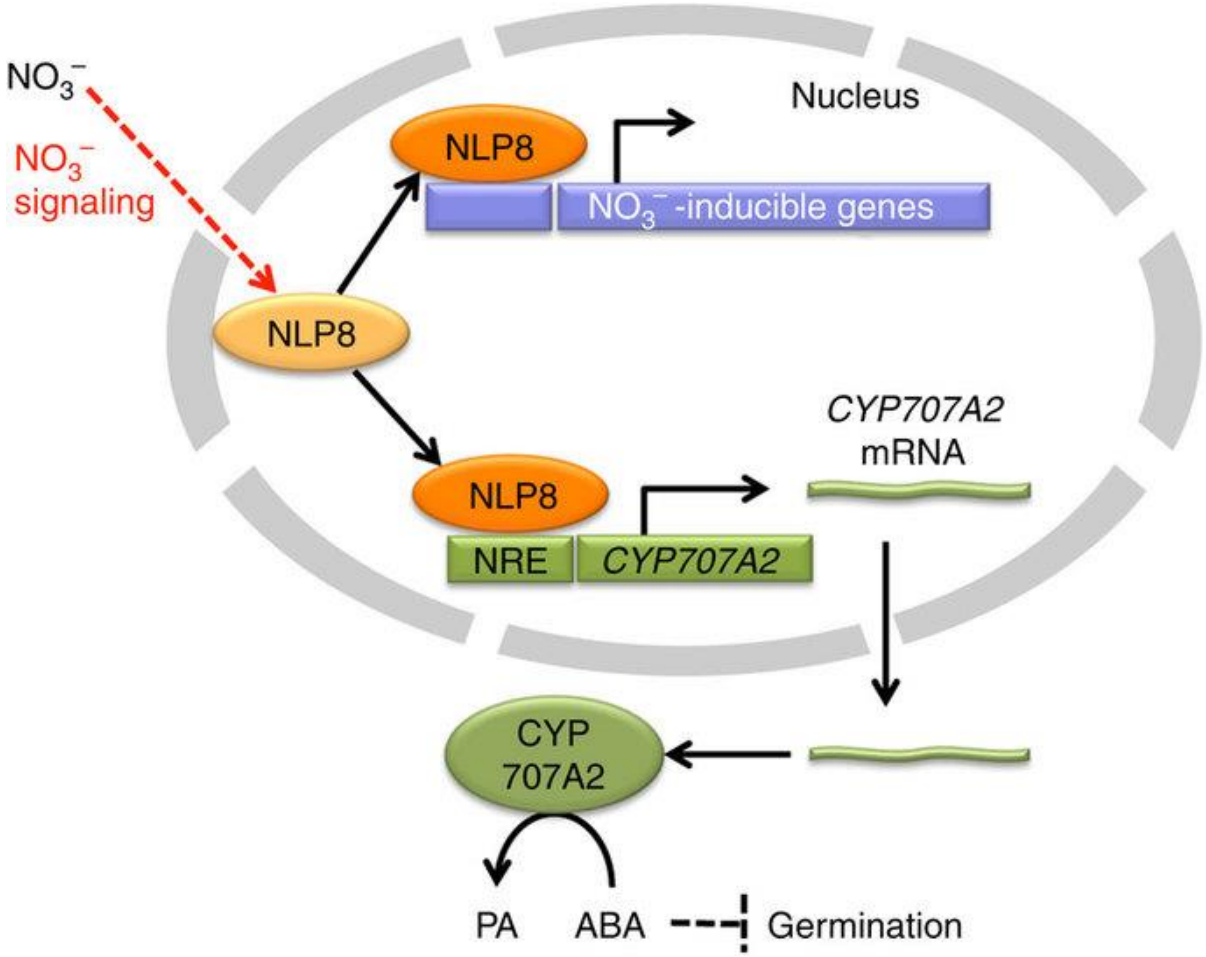

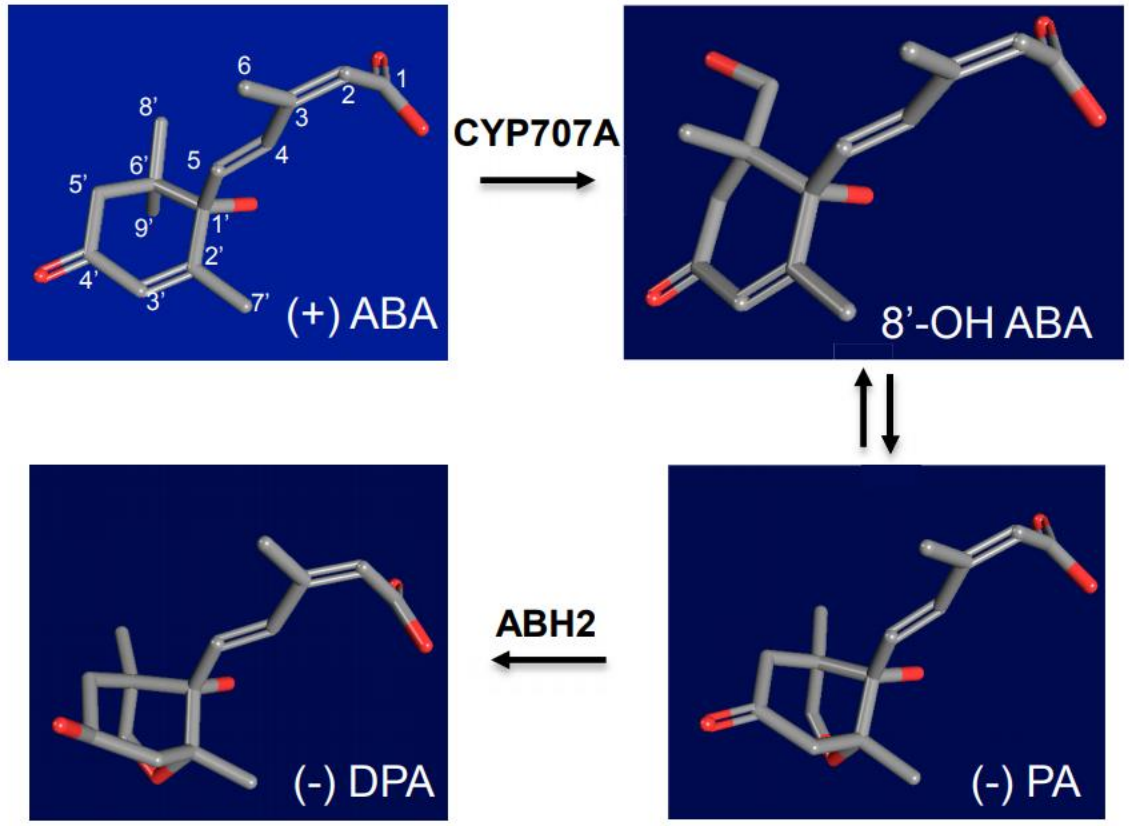

Figure 1. Catabolism of ABA through the 8′-Hydroxylation Pathway.
Cyclization of 8′-OH ABA into PA is a reversible reaction under abiotic conditions; however, under *in vivo* conditions 8′-OH spontaneously (and/or enzymatically) isomerizes to PA. ABA, abscisic acid; 8′-OH ABA, 8′-hydroxy ABA; PA, phaseic acid; DPA, dihydrophaseic acid; CYP707A, CYP707A family cytochrome P450 mono-oxygenases; ABH2, PA reductase.

Journal of Experimental Botany, Vol. 57, No. 3, pp. 517–526, 2006
doi:10.1093/jxb/erj060 Advance Access publication 23 December, 2005

Journal of Experimental Botany

FOCUS PAPER

Nitric oxide reduces seed dormancy in *Arabidopsis*

Paul C. Bethke*, Igor G. L. Libourel and Russell L. Jones

<u>SCAVENGER of NO</u>

cPTIO = 2-(4-Carboxyphenyl)-4,4,5,5-tetramethylimidazoline-1-oxyl-3-oxide potassium salt

NO PRODUCER

SNP = Sodium nitroprusside

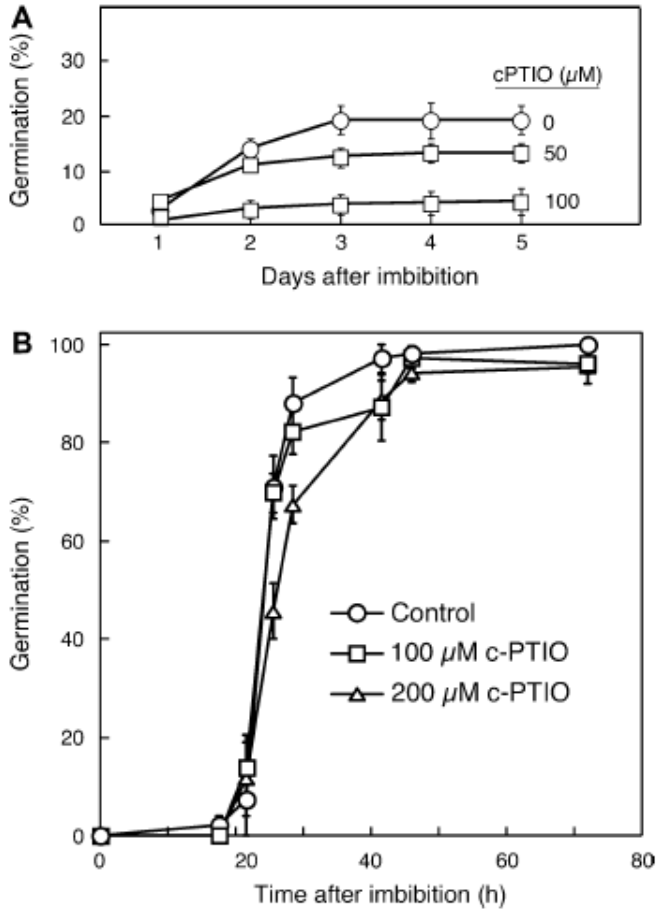

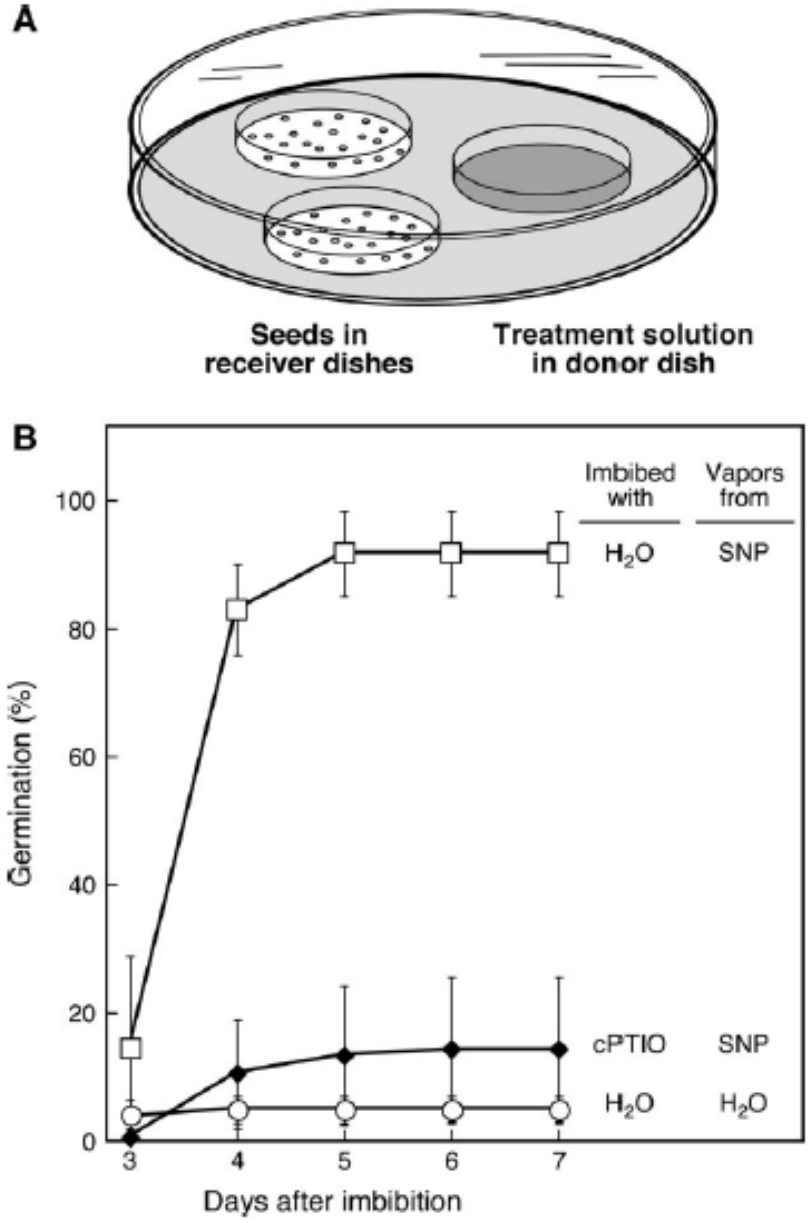

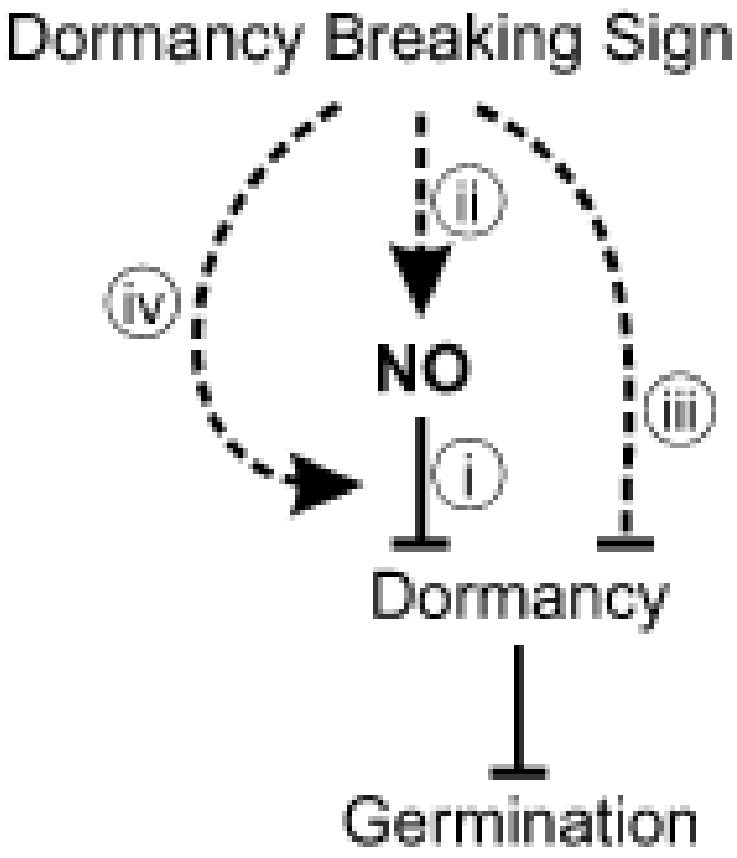

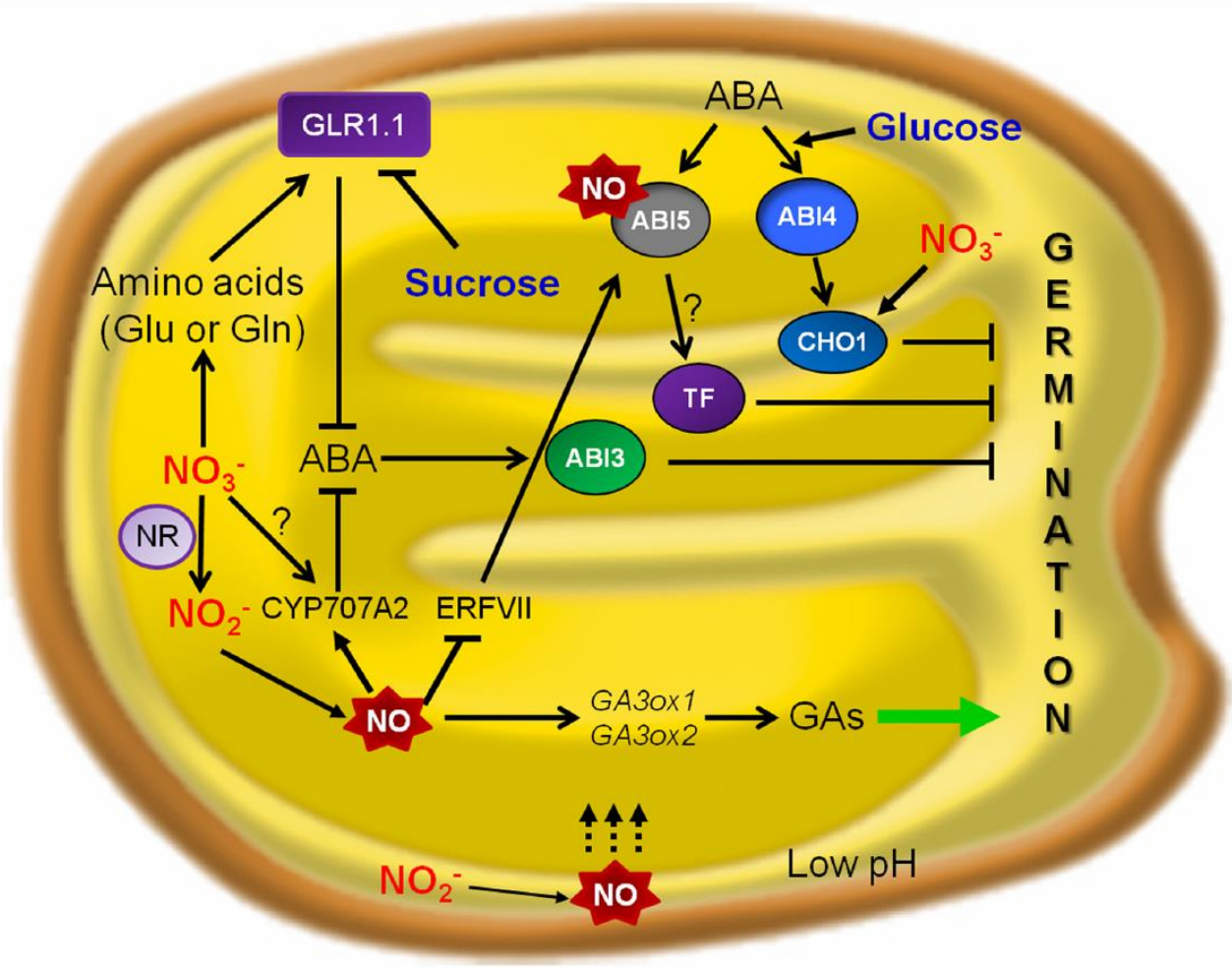

NO has also a strong effect in releasing seed dormancy

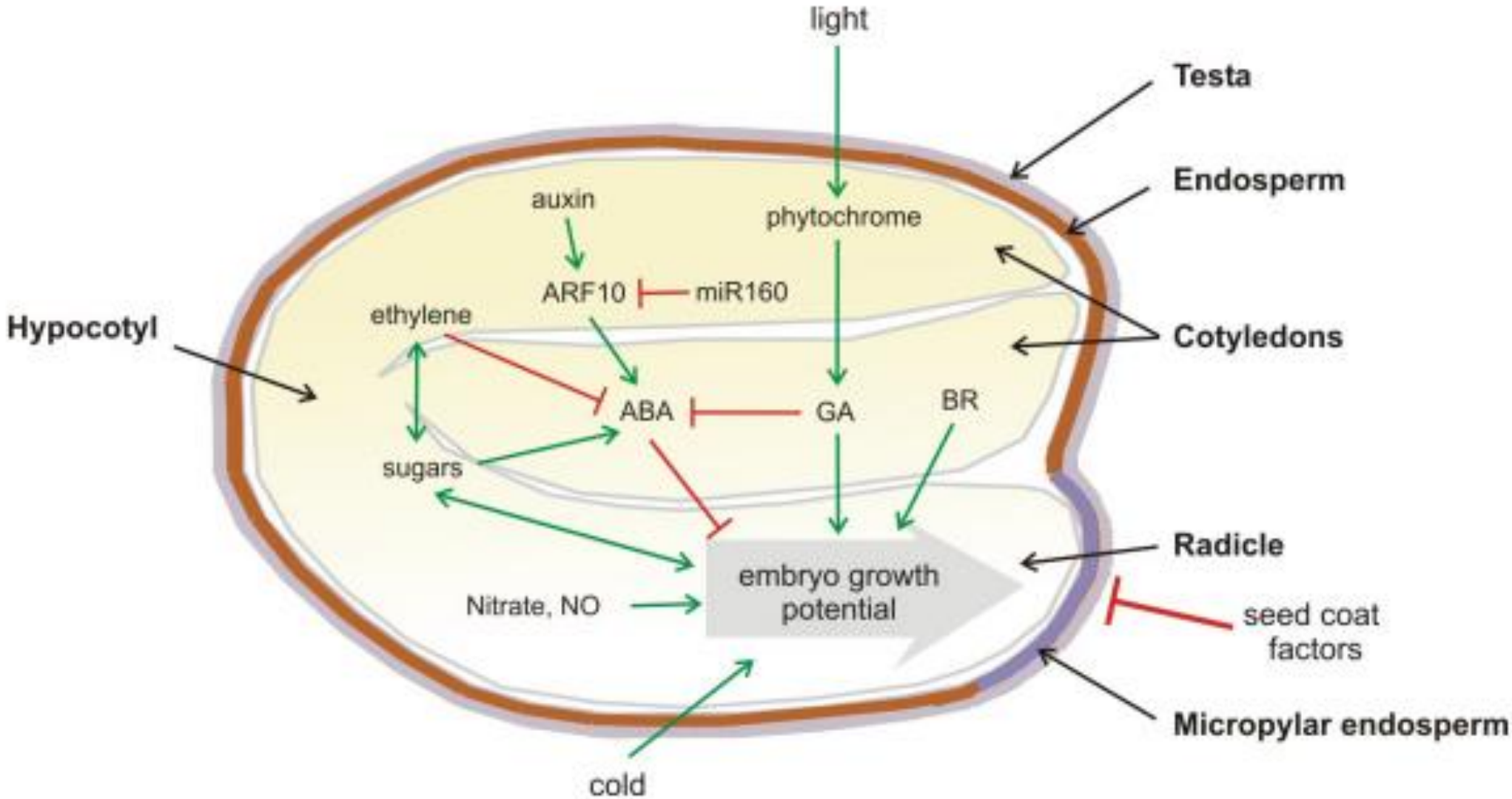
light
Testa
Endosperm
auxin
phytochrome
ARF10
miR160
ethylene
Hypocotyl
Cotyledons
ABA
GA
BR
sugars
Radicle
embryo growth
potential
Nitrate, NO
seed coat
factors
Micropylar endosperm
cold

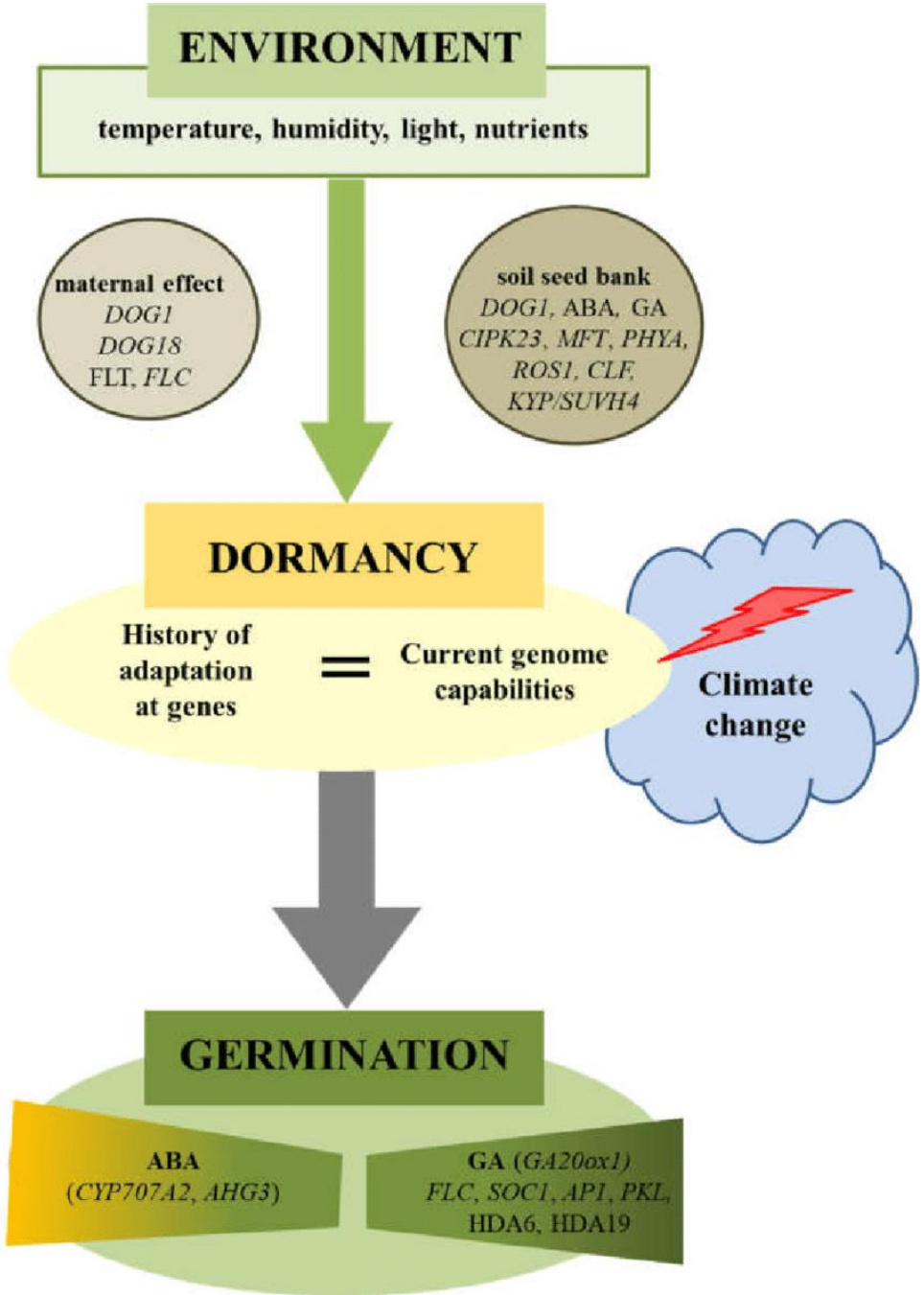

International Journal of *Molecular Sciences*

MDPI

Review

Regulation of Seed Dormancy and Germination Mechanisms in a Changing Environment

Ewelina A. Klupczyńska and Tomasz A. Pawłowski *

The Plant Cell, Vol. 32: 2094–2119, July 2020, www.plantcell.org © 2020 ASPB.

REVIEW

Nitrate in 2020: Thirty Years from Transport to Signaling Networks

Elena A. Vidal,[a,b,c] José M. Alvarez,[a,b,d] Viviana Araus,[d] Eleodoro Riveras,[a,e,f] Matthew D. Brooks,[d] Gabriel Krouk,[g] Sandrine Ruffel,[g] Laurence Lejay,[g] Nigel M. Crawford,[h] Gloria M. Coruzzi,[d] and Rodrigo A. Gutiérrez[a,e,f,1]

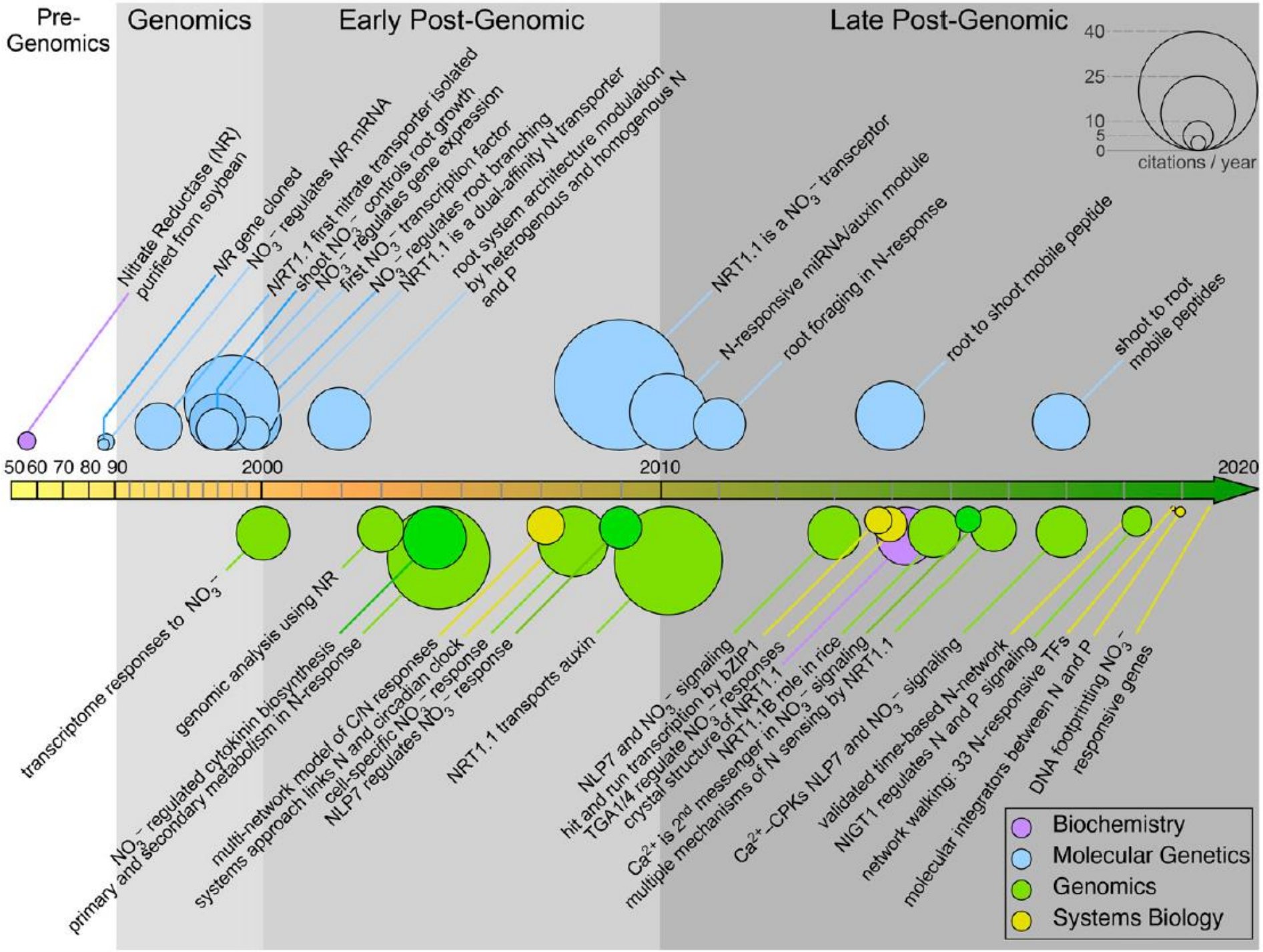

NRT1.1 nitrate transporter

Developmental Cell
Article

Nitrate-Regulated Auxin Transport by NRT1.1 Defines a Mechanism for Nutrient Sensing in Plants

Gabriel Krouk,[1,5] Benoît Lacombe,[1] Agnieszka Bielach,[2] Francine Perrine-Walker,[1] Katerina Malinska,[3] Emmanuelle Mounier,[1] Klara Hoyerova,[3] Pascal Tillard,[1] Sarah Leon,[1] Karin Ljung,[4] Eva Zazimalova,[3] Eva Benkova,[2] Philippe Nacry,[1] and Alain Gojon[1,*]

Figure 1. Nitrate Dependence of Increased Auxin Accumulation in Lateral Root Primordia and Young Lateral Roots Resulting from *NRT1.1* Mutation

(A) Histochemical staining of GUS activity in lateral root primordia and newly emerged lateral roots of transgenic *Arabidopsis* plants expressing *DR5::GUS* in wild-type or *chl1-5* background. Three stages of development are considered: initiating primordia (a), primordia prior to emergence (b), and newly emerged lateral roots (c). The plants were cultivated for 8 days on media containing nitrogen sources described in the figure.

(B) IAA immunolocalization in LR tips of wild-type and *chl1-5* plants. The IAA signal (dark area) in the LR tip is indicated by the arrowheads. The pictures shown are representative of 13 and 34 independent replicates for Col and *chl1-5* seedlings, respectively. See also Figure S1.

NITRATE TRANPORTER LOWER AUXIN ACCUMULATION IN ROOT PRIMORDIA

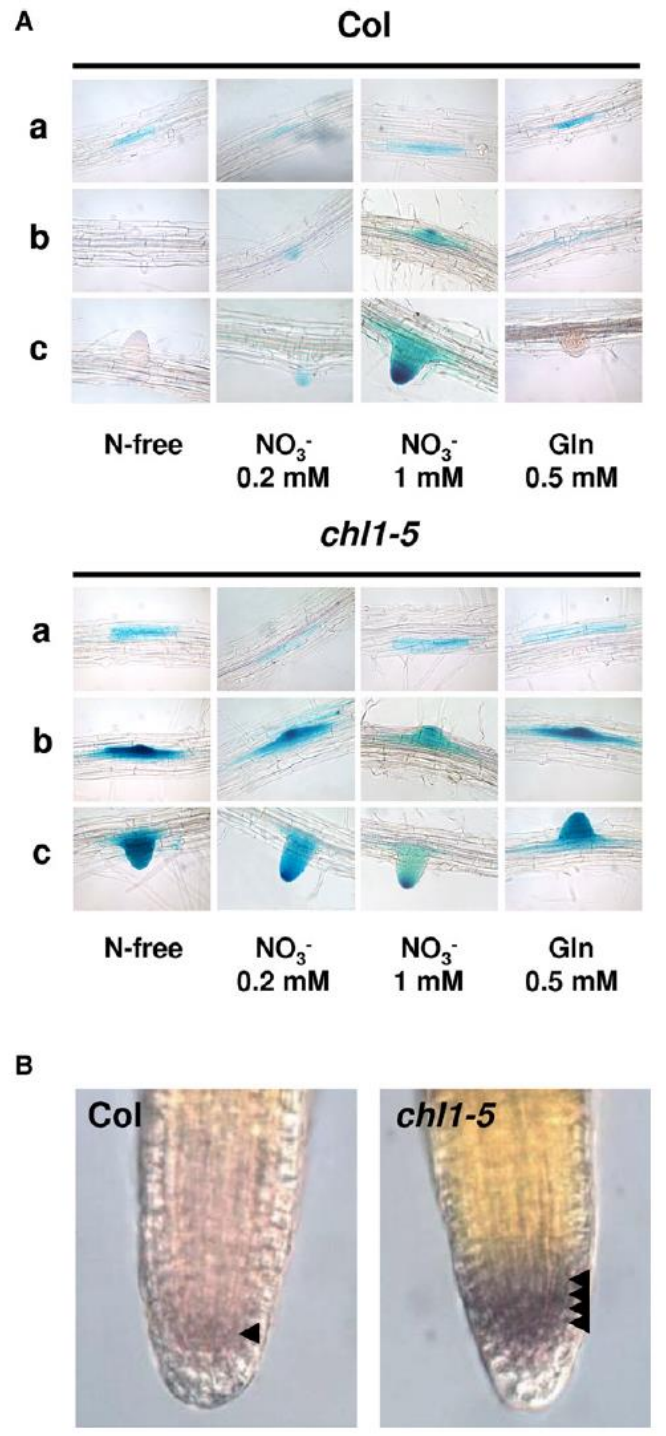

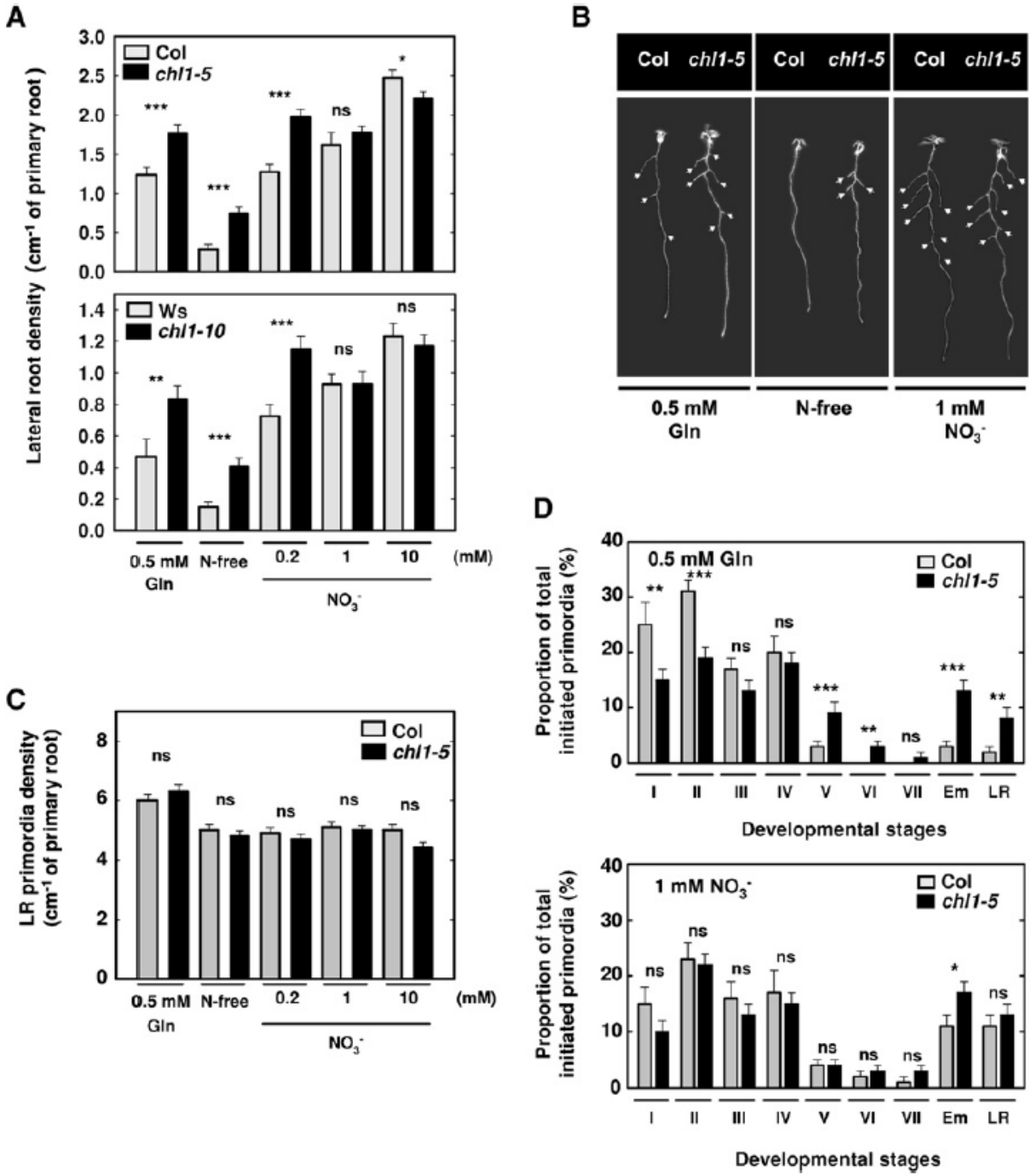

Figure 2. *chl1* Mutation Promotes Lateral Root Growth in the Absence or at Low Concentration of NO_3^-

(A) Density of visible (>0.5 mm) lateral roots in plants (Col, *chl1-5*, Ws, *chl1-10*) grown for 8 days on media containing nitrogen sources described in the figure. Results (n = 30–52) are representative of three independent experiments. Differences between mutant and wild-type genotypes are statistically significant at $^*p < 0.05$; $^{**}p < 0.01$; $^{***}p < 0.001$ (t test). ns, not significant.

(B) Selected pictures figuring *chl1-5* root phenotype. Arrowheads indicate visible lateral roots.

(C) Density of lateral root primordia initiated on the primary root of Col and *chl1-5* plants grown for 8 days on media containing nitrogen sources described in the figure (n = 20).

(D) Distribution of lateral root primordia between various stages of development (Em, emerged primordia; LR, lateral root) in Col and *chl1-5* plants grown either on 0.5 mM glutamine or 1 mM NO_3^- as an N source. Results (n = 20) are expressed as the proportion of total lateral root primordia initiated.

Differences between mutant and wild-type genotypes are statistically significant at $^*p < 0.05$; $^{**}p < 0.01$; $^{***}p < 0.001$ (t test). ns, not significant. See also Figure S2.

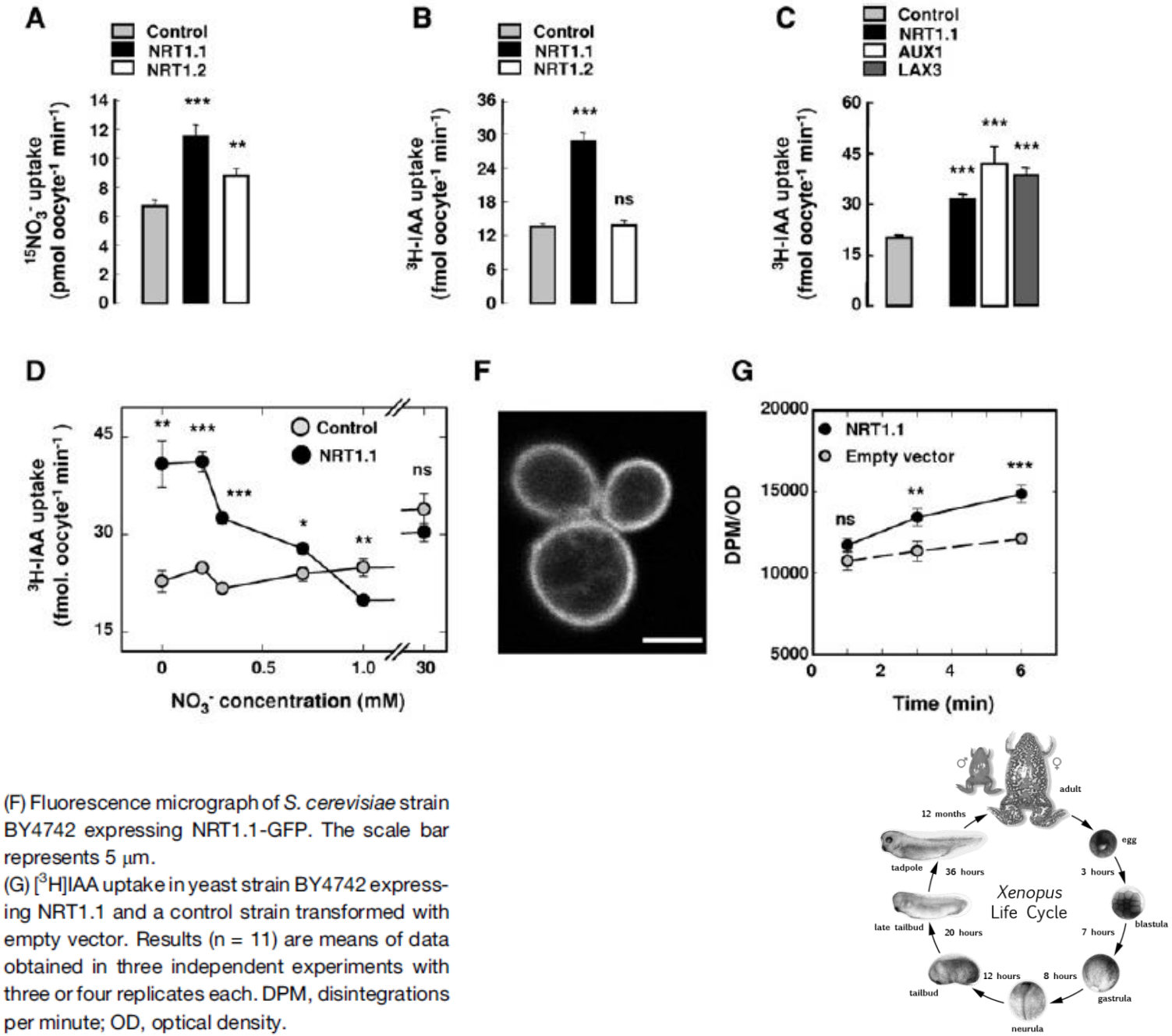

(F) Fluorescence micrograph of *S. cerevisiae* strain BY4742 expressing NRT1.1-GFP. The scale bar represents 5 μm.

(G) [^{3}H]IAA uptake in yeast strain BY4742 expressing NRT1.1 and a control strain transformed with empty vector. Results (n = 11) are means of data obtained in three independent experiments with three or four replicates each. DPM, disintegrations per minute; OD, optical density.

Figure 3. NRT1.1 Facilitates NO_3^--Inhibited Auxin Influx in Heterologous Expression Systems and In Planta

(A) $^{15}NO_3^-$ uptake in NRT1.1-cRNA- or NRT1.2-cRNA-injected and control *Xenopus* oocytes supplied with 30 mM $^{15}NO_3^-$. Results (n = 6 batches of five oocytes) are representative of five and three independent experiments for NRT1.1 and NRT1.2, respectively (each experiment was performed with oocytes from a different frog). Data were analyzed through one-way ANOVA, three-level factor (control; NRT1.1; NRT1.2), p = 9.0 e-06, followed by a t test as a post hoc analysis.

(B) [^{3}H]IAA uptake in NRT1.1-cRNA- or NRT1.2-cRNA-injected and control *Xenopus* oocytes supplied with 1 μM [^{3}H]IAA. Results (n = 24–30) are representative of five and three independent experiments for NRT1.1 and NRT1.2, respectively (each experiment was performed with oocytes from a different frog). Data were analyzed through one-way ANOVA, three-level factor (control; NRT1.1; NRT1.2), p = 2.2 e-16, followed by a t test as a post hoc analysis.

(C) [^{3}H]IAA uptake in NRT1.1-cRNA-, AUX1-cRNA-, and LAX3-cRNA-injected and control *Xenopus* oocytes supplied with 1 μM [^{3}H]IAA (n = 7–18).

(D) Effect of increasing NO_3^- concentration on [^{3}H]IAA uptake in NRT1.1-cRNA-injected and control *Xenopus* oocytes supplied with 1 μM [^{3}H]IAA (n = 8–22).

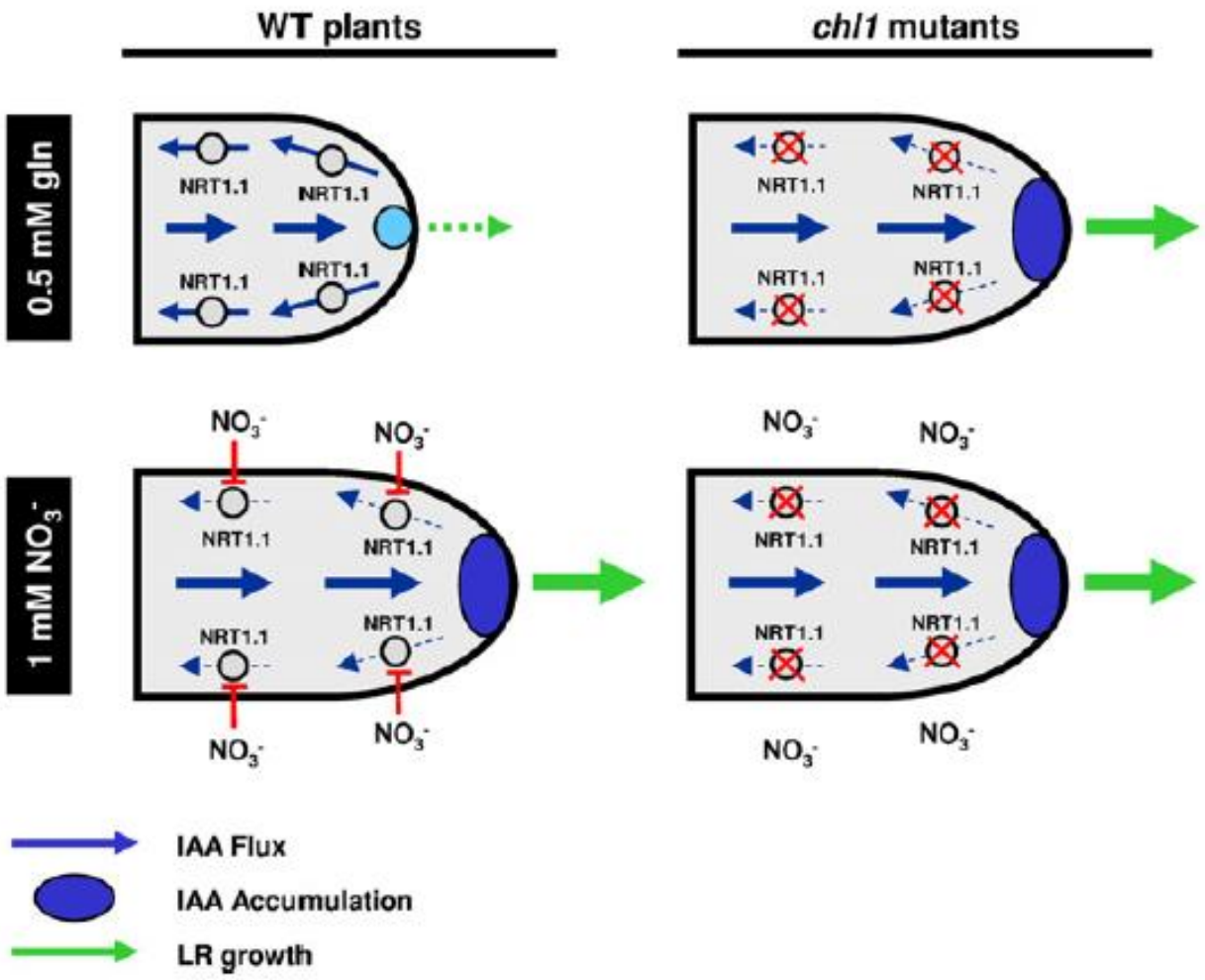

Figure 5. Schematic Model for NRT1.1 Control of Lateral Root Growth in Response to Nitrate

Two situations are shown to illustrate the specific effect of NO_3^- on lateral root growth, corresponding to plants supplied either with 0.5 mM glutamine or with 1 mM NO_3^- (1 mM external N in both cases). The model postulates that in the absence of NO_3^- (glutamine-fed plants), NRT1.1 favors basipetal transport of auxin in lateral roots, thus preventing auxin accumulation at the lateral root tip. This slows down outgrowth and elongation of lateral roots. At 1 mM NO_3^-, facilitation of basipetal auxin transport by NRT1.1 is inhibited, leading to auxin accumulation in the lateral root tip and accelerated growth of lateral root. Accordingly, *NRT1.1* mutation in *chl1* plants, which suppresses facilitation of basipetal auxin transport by NRT1.1, results in high auxin levels in the lateral root tip and accelerated growth of lateral roots, regardless of the external N source. Direct basipetal auxin transport by NRT1.1 is shown for simplicity to illustrate its facilitation of this transport flow.

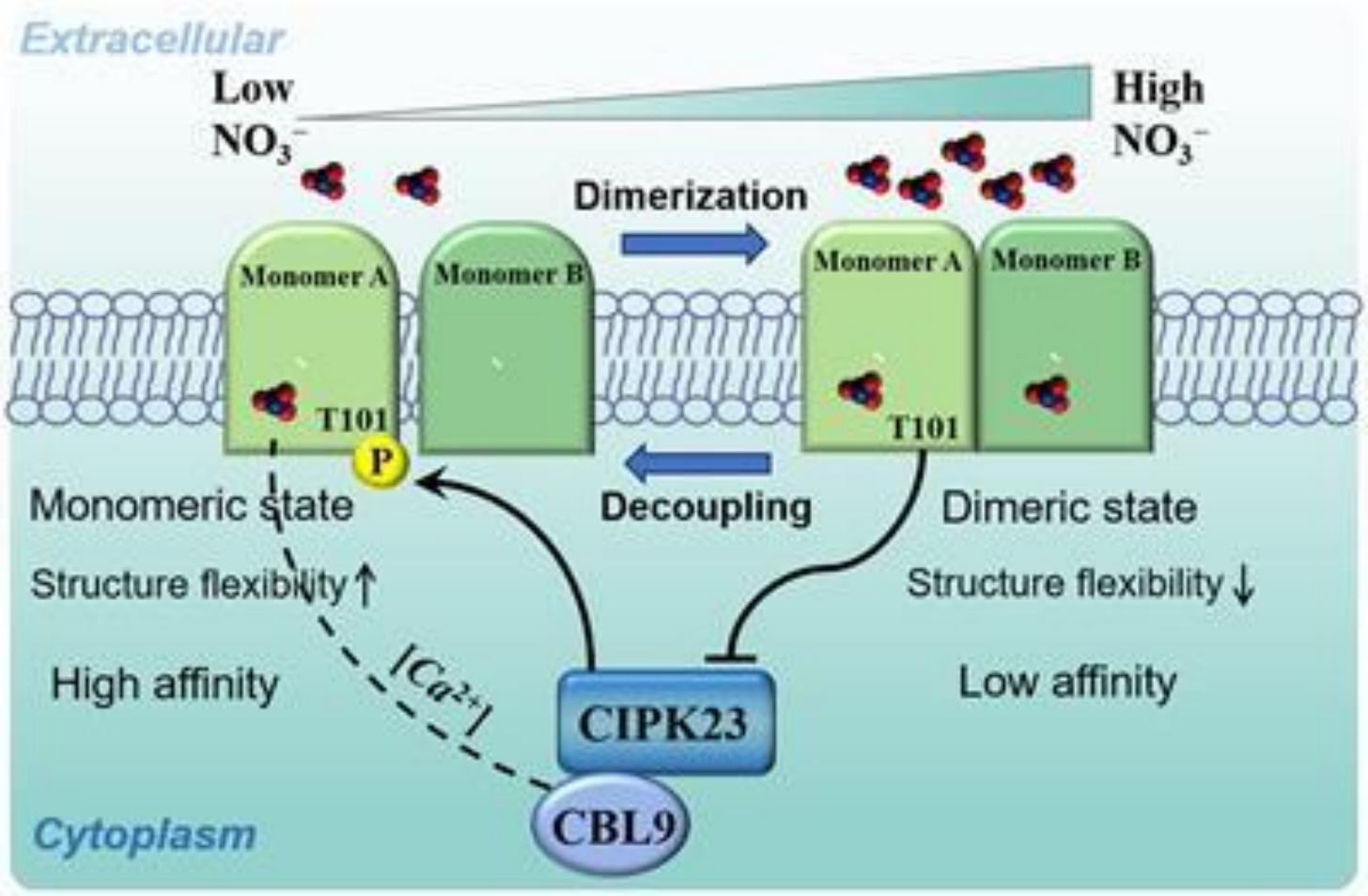

NRT1.1 a dual affinity transporter

ARTICLE

doi:10.1038/nature13074

Crystal structure of the plant dual-affinity nitrate transporter NRT1.1

Ji Sun[1], John R. Bankston[2], Jian Payandeh[1]†, Thomas R. Hinds[1], William N. Zagotta[2] & Ning Zheng[1,3]

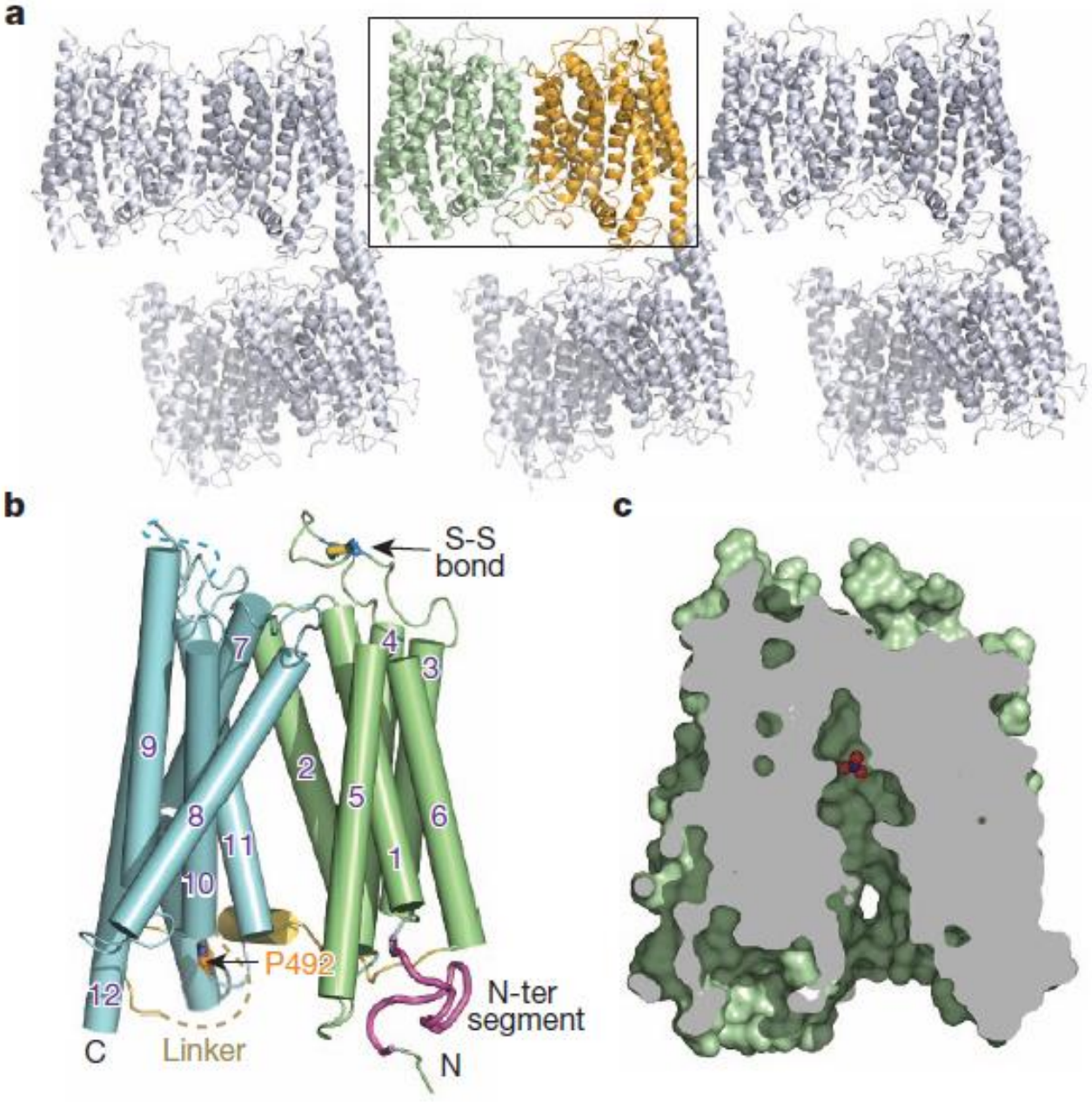

Figure 1 | Crystal packing and overall structure of NRT1.1. **a**, Crystal packing of NRT1.1 in space group *C*2221 with two molecules in each asymmetric unit. **b**, Overall structure of NRT1.1. The N-terminal and C-terminal domains, the N-terminal conserved segment, the inter-domain linker and Pro 492 are coloured in pale green, cyan, magenta, yellow and orange, respectively. A functional important extracellular disulphide bond is indicated. **c**, Cutaway view showing that NRT1.1 is captured in an inward conformation with nitrate displayed as spheres.

DIMER CONFORMATION, WITH EACH N-TERMINAL HALF FACING AND INTERACTING WITH EACH OTHER

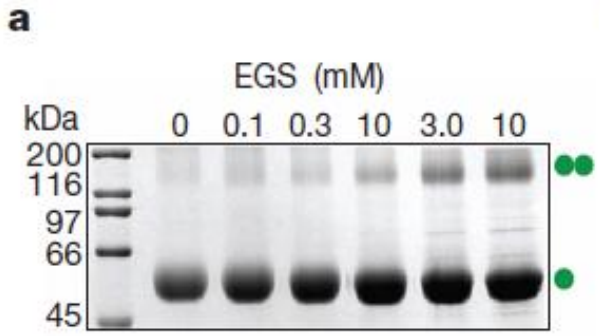

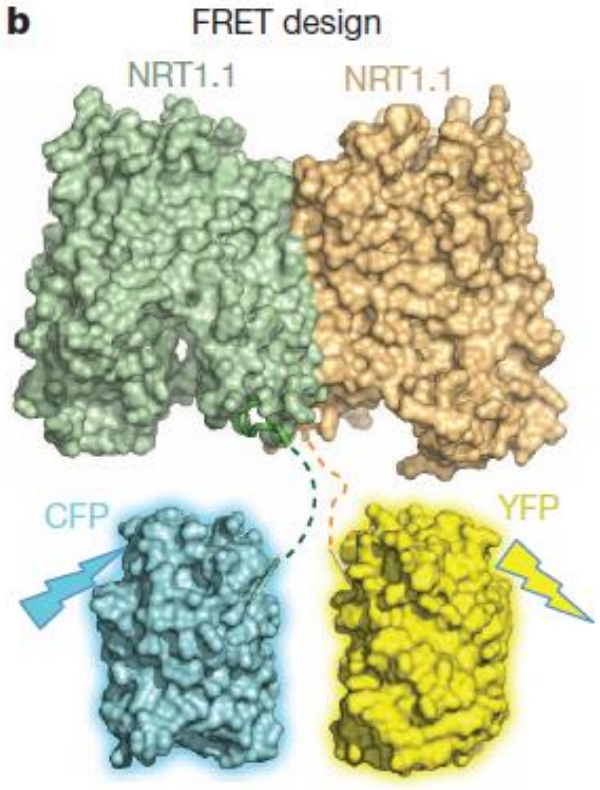

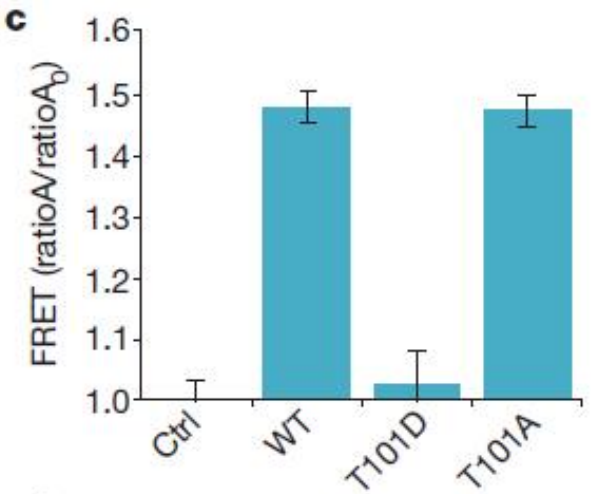

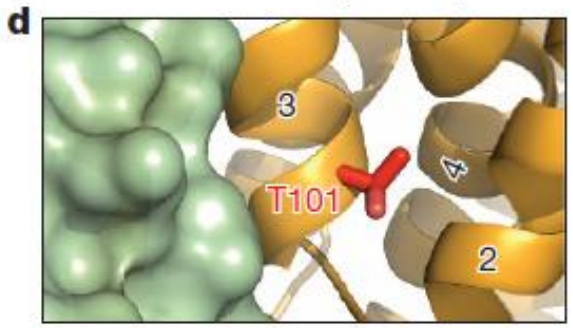

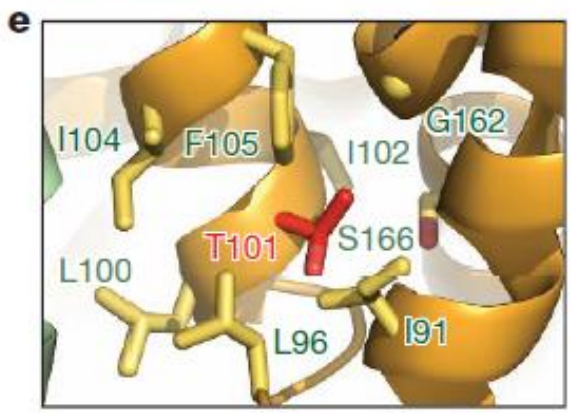

UNMODIFIED NRT1.1 THEREFORE ADOPTS A DIMER CONFIGURATION SUITABLE FOR LOWAFFINITY NITRATE UPTAKE, WHILE LOW N-MEDIATED PHOSPHORYLATION AT THR-101 TRIGGERS CONVERSION TO A MONOMER WITH HIGHER STRUCTURE FLEXIBILITY, WHICH MIGHT EXPLAIN THE SWITCH TO HIGH AFFINITY

Figure 3 | NRT1.1 dimerization controlled by Thr 101 phosphorylation. **a**, Crosslinking of NRT1.1 with increasing concentrations of ethylene glycol bis-succinimidylsuccinate (EGS). **b**, The design of FRET assay. Dashed lines indicate the 11-residue-long linkers between the fluorescence proteins and the structurally resolved NRT1.1 N terminus. **c**, FRET measurements of wild-type (WT) and mutant NRT1.1. The mCFP–HCN–mYFP–NRT1.1 pair was used as negative control. Consistent with the loss of FRET signal, the T101D mutant failed to be crosslinked in solution (Extended Data Fig. 5b). **d**, A close-up view of Thr 101 at the NRT1.1 dimer interface. **e**, Thr 101-interacting residues with their side chains shown as sticks.

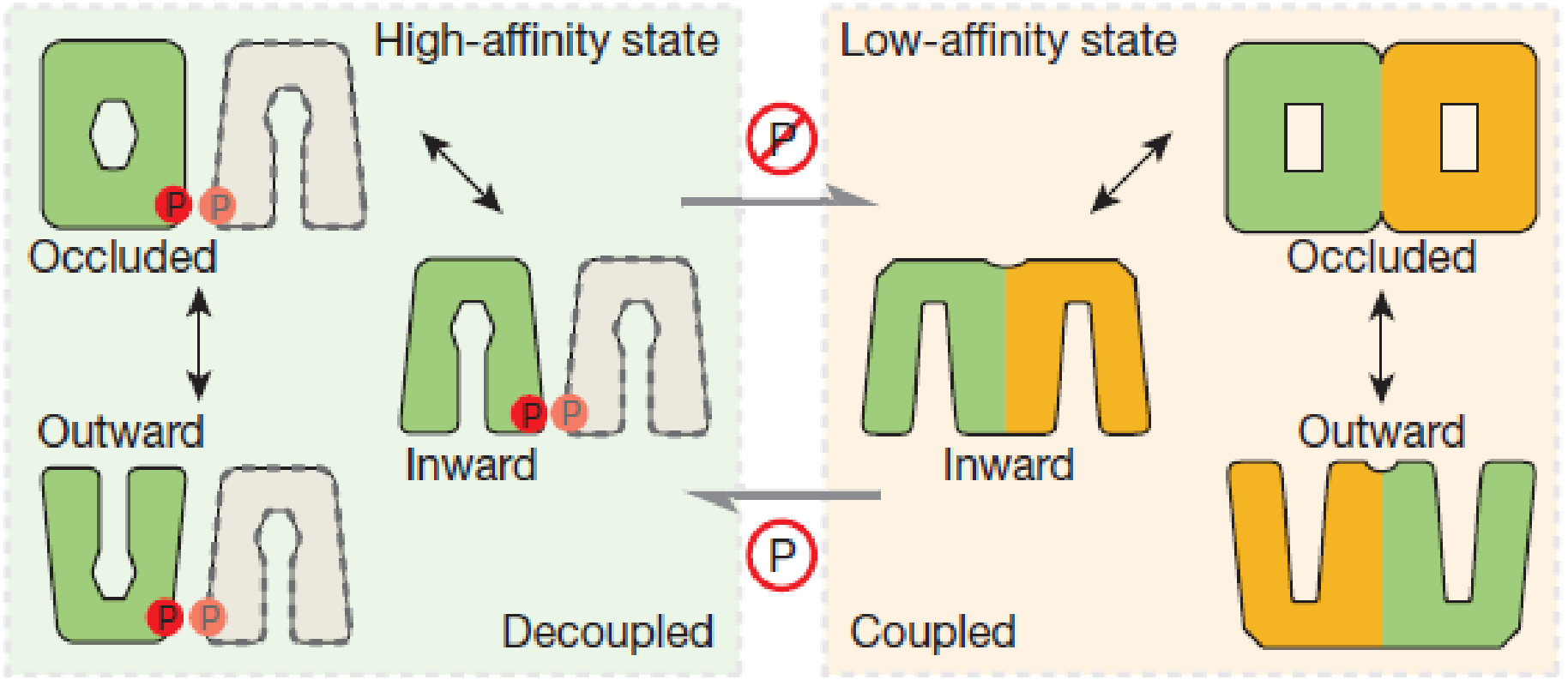

Figure 5 | A dimerization switch model. The non-phosphorylated and structurally coupled NRT1.1 dimer functions as an 'in-phase' homodimeric low-affinity nitrate transporter (right). Once phosphorylated, the NRT1.1 dimer is decoupled, and each molecule functions as an independent high-affinity nitrate transporter (left). Different shapes of the putative substrate-binding site at the central transport tunnel reflect its differential nitrate-binding properties.

Cell

CHL1 Functions as a Nitrate Sensor in Plants

Cheng-Hsun Ho,[1,2] Shan-Hua Lin,[2] Heng-Cheng Hu,[2] and Yi-Fang Tsay[1,2,*]
[1]Molecular Cell Biology, Taiwan International Graduate Program, Institute of Molecular Biology, Academia Sinica, and Graduate Institute of Life Sciences, National Defense Medical Center, Taipei, Taiwan
[2]Institute of Molecular Biology, Academia Sinica, Taipei 115, Taiwan
*Correspondence: yftsay@gate.sinica.edu.tw
DOI 10.1016/j.cell.2009.07.004

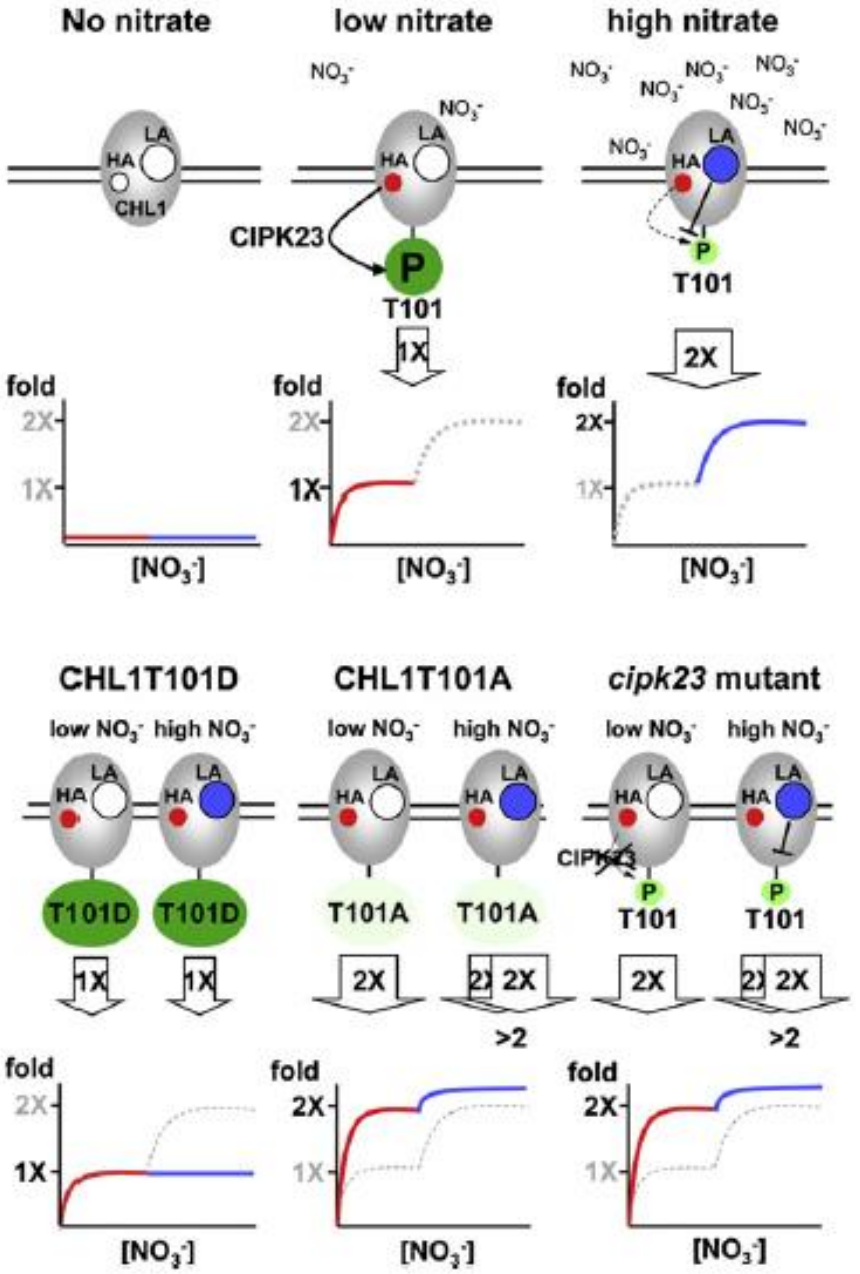

Figure 7. Schematic Model for CIPK23- and CHL1-Mediated Nitrate Sensing in the Primary Nitrate Response

The top panel shows the nitrate sensing mechanism, while the bottom panel shows gene expression during the primary nitrate response. The gray ovals represent CHL1 in the plasma membrane. The small and large empty circles represent the high- and low-affinity nitrate binding sites, respectively. The red and blue circles indicate nitrate binding to the high- and low-affinity binding site, respectively. P denotes phosphorylated CHL1T101 and the green color gradient represents the level of CHL1T101 phosphorylation. The panels below the cartoons represent the level of gene expression in the primary nitrate response, with red for the high-affinity phase and blue for the low-affinity phase.

nature plants
LETTERS
PUBLISHED: 2 MARCH 2015 | ARTICLE NUMBER: 15015 | DOI: 10.1038/NPLANTS.2015.15

Multiple mechanisms of nitrate sensing by *Arabidopsis* nitrate transceptor NRT1.1

E. Bouguyon[1], F. Brun[1], D. Meynard[2], M. Kubeš[3], M. Pervent[1], S. Leran[1], B. Lacombe[1], G. Krouk[1], E. Guiderdoni[2], E. Zažímalová[3], K. Hoyerová[3], P. Nacry[1] and A. Gojon[1]*

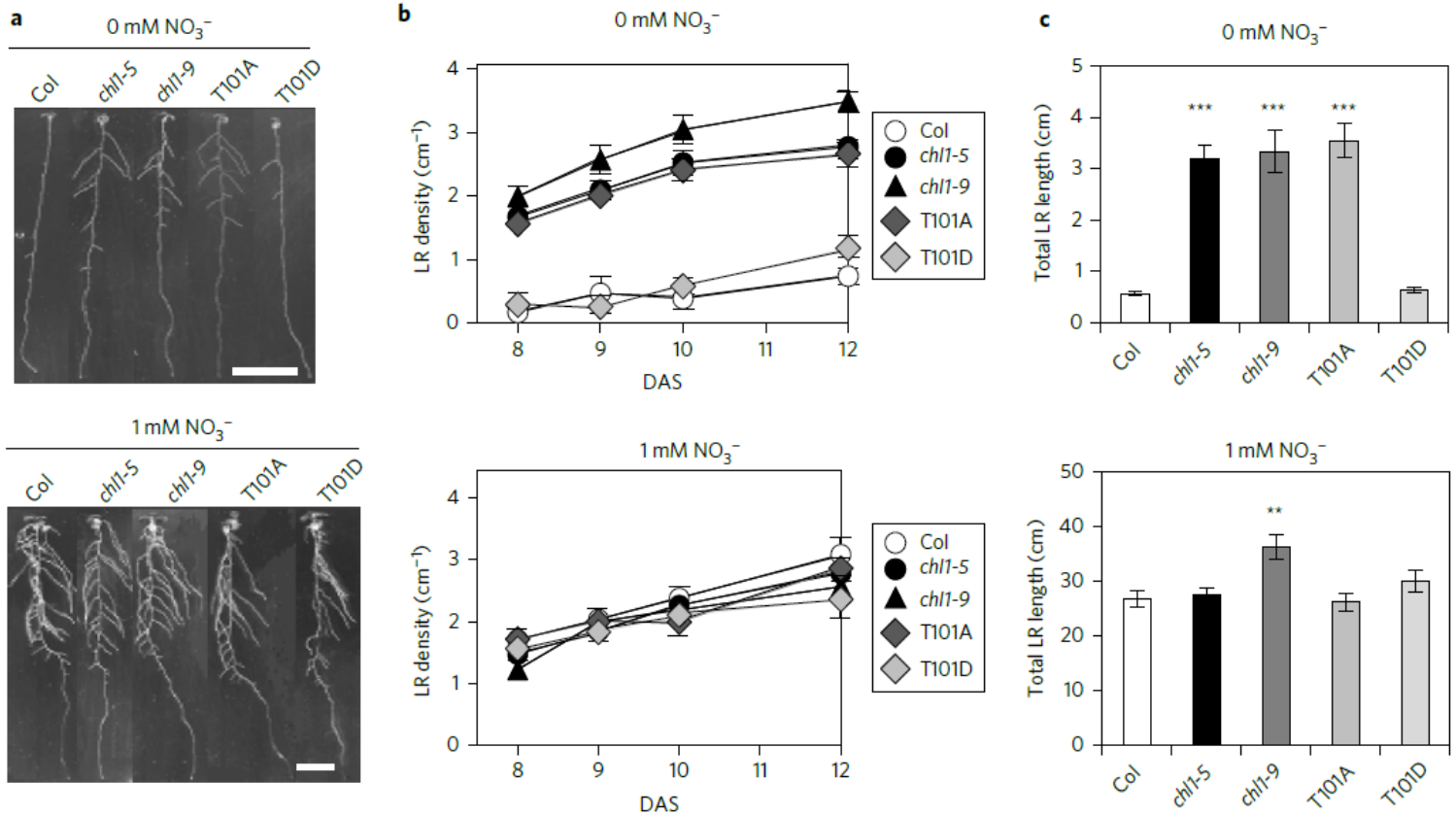

Figure 1 | Point mutations in the NRT1.1 nitrate transceptor differentially alter the nitrate regulation of lateral root growth. NRT1.1-dependent inhibition of lateral root development in the absence of NO_3^- is defective in *chl1-5*, *chl1-9* and T101A plants, but not in T101D plants. **a**, Plants grown for 12 days on NO_3^--free medium or on medium containing 1 mM NO_3^-. **b**, Lateral root density (number of visible lateral roots per cm of primary root) between 8 and 12 days after sowing (DAS). **c**, Total lateral root length at day 12. Data ($n = 30$–50) are mean ± s.e. from three independent experiments. Differences from the WT (Col) are statistically significant at $^{**}P < 0.01$ or $^{***}P < 0.001$. Scale bars, 1 cm.

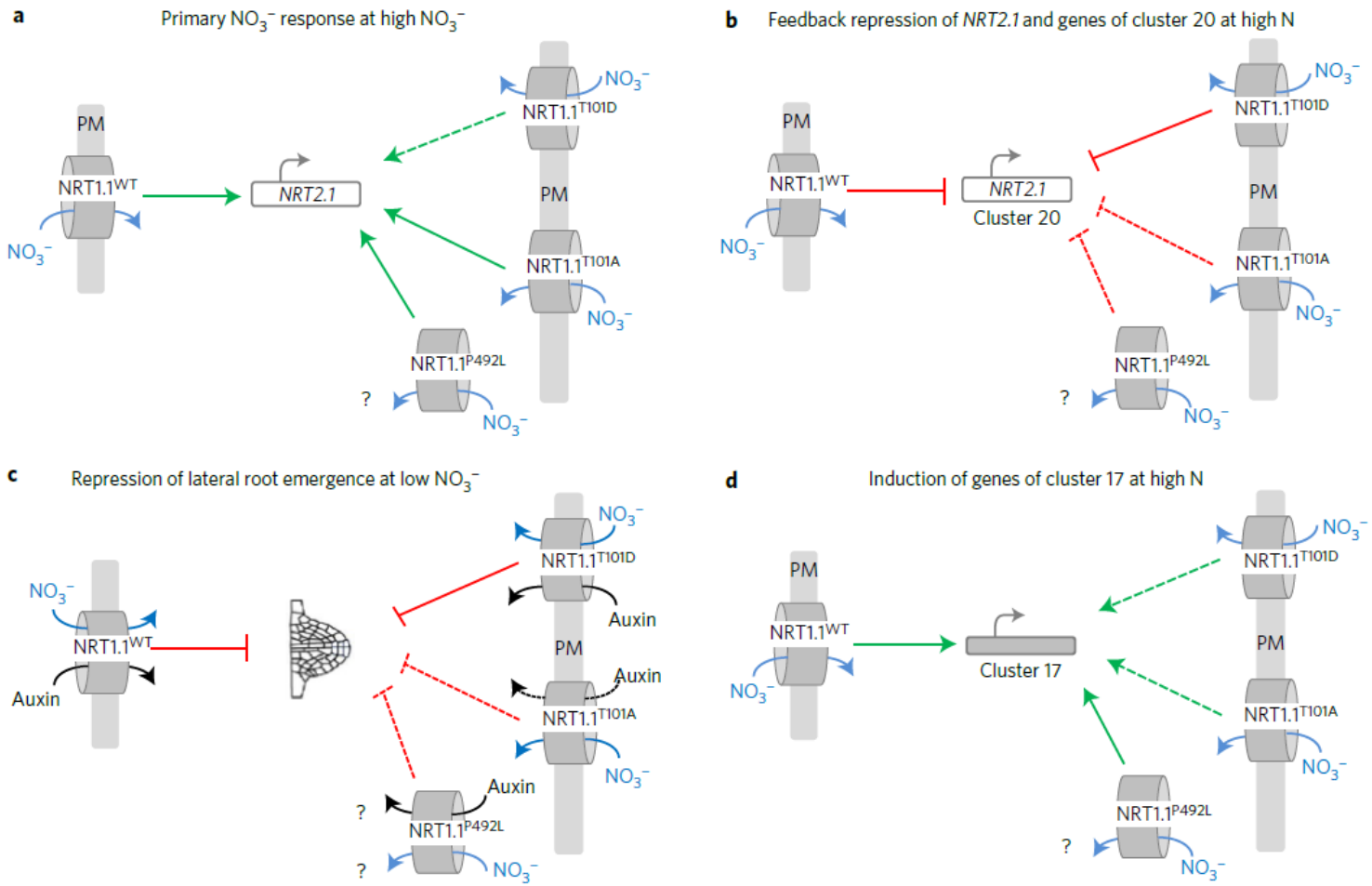

Figure 6 | Schematic representation of the four signalling 'modes' of NRT1.1. The four panels illustrate the NRT1.1-dependent responses to NO_3^- investigated in this work ($NRT1.1^{WT}$ is on the left side of each panel), and the effect of point mutations in NRT1.1 on these responses (right side of each panel). **a**, Primary nitrate response at high NO_3^- with induction of *NRT2.1* as a marker. **b**, Feedback repression of *NRT2.1* and genes of cluster 20 by high nitrogen concentration (the same pattern holds true for genes of clusters 11 and 16, but with induction instead of repression). **c**, Repression of lateral root emergence at low NO_3^-. **d**, Induction of genes of cluster 17 by high N (the same pattern holds true for genes of clusters 13, but with repression instead of induction). Green and red lines represent induction and repression, respectively. Plain lines represent normal responses as recorded for $NRT1.1^{WT}$. Dotted lines represent attenuated or suppressed responses as compared to $NRT1.1^{WT}$. $NRT1.1^{P492L}$ is not pictured in the plasma membrane to illustrate the predominant intracellular localization of the $NRT1.1^{P492L}$::mCherry protein. Auxin transport by NRT1.1 is only shown at low NO_3^- because this transport is inhibited at high NO_3^- (ref. 19).

Stratification

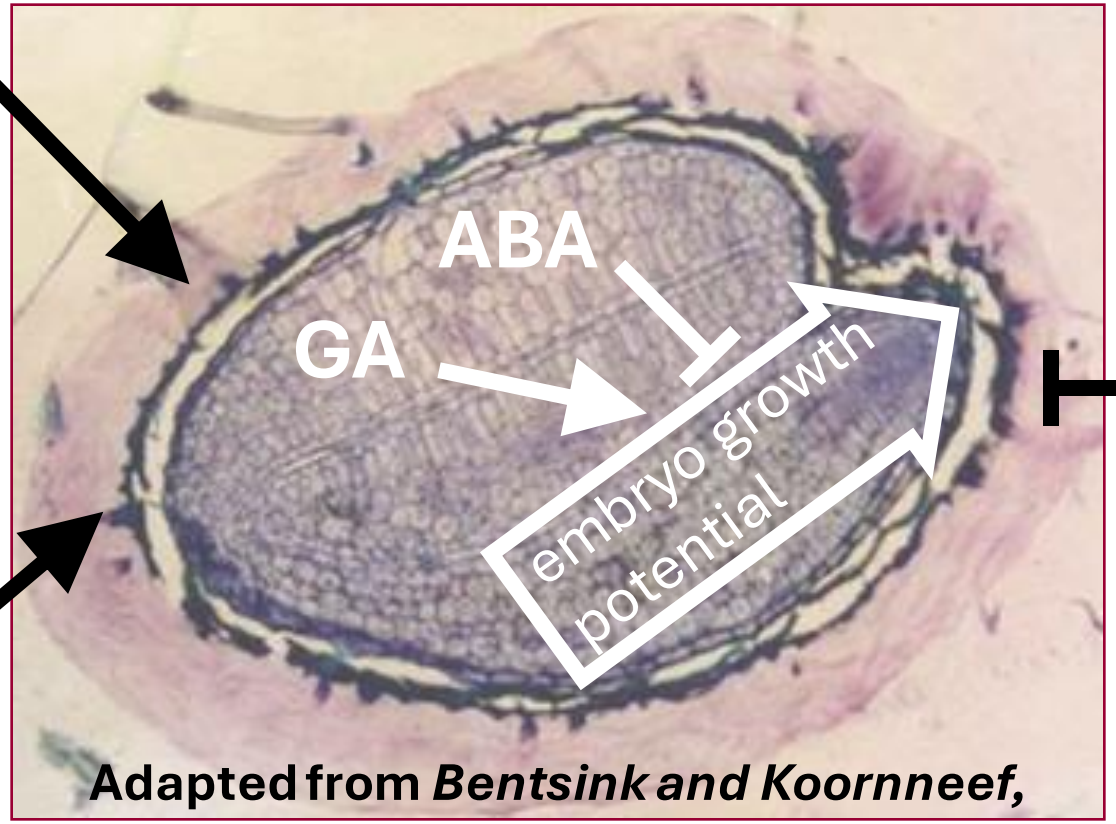

seed coat factors

KNO_3, GAs…

Adapted from ***Bentsink and Koornneef, 2002***

Seed coats and transparent testa mutants

Plant Physiology, February 2000, Vol. 122, pp. 403–413, www.plantphysiol.org © 2000 American Society of Plant Physiologists

Influence of the Testa on Seed Dormancy, Germination, and Longevity in Arabidopsis[1]

Isabelle Debeaujon[2], Karen M. Léon-Kloosterziel[3], and Maarten Koornneef*

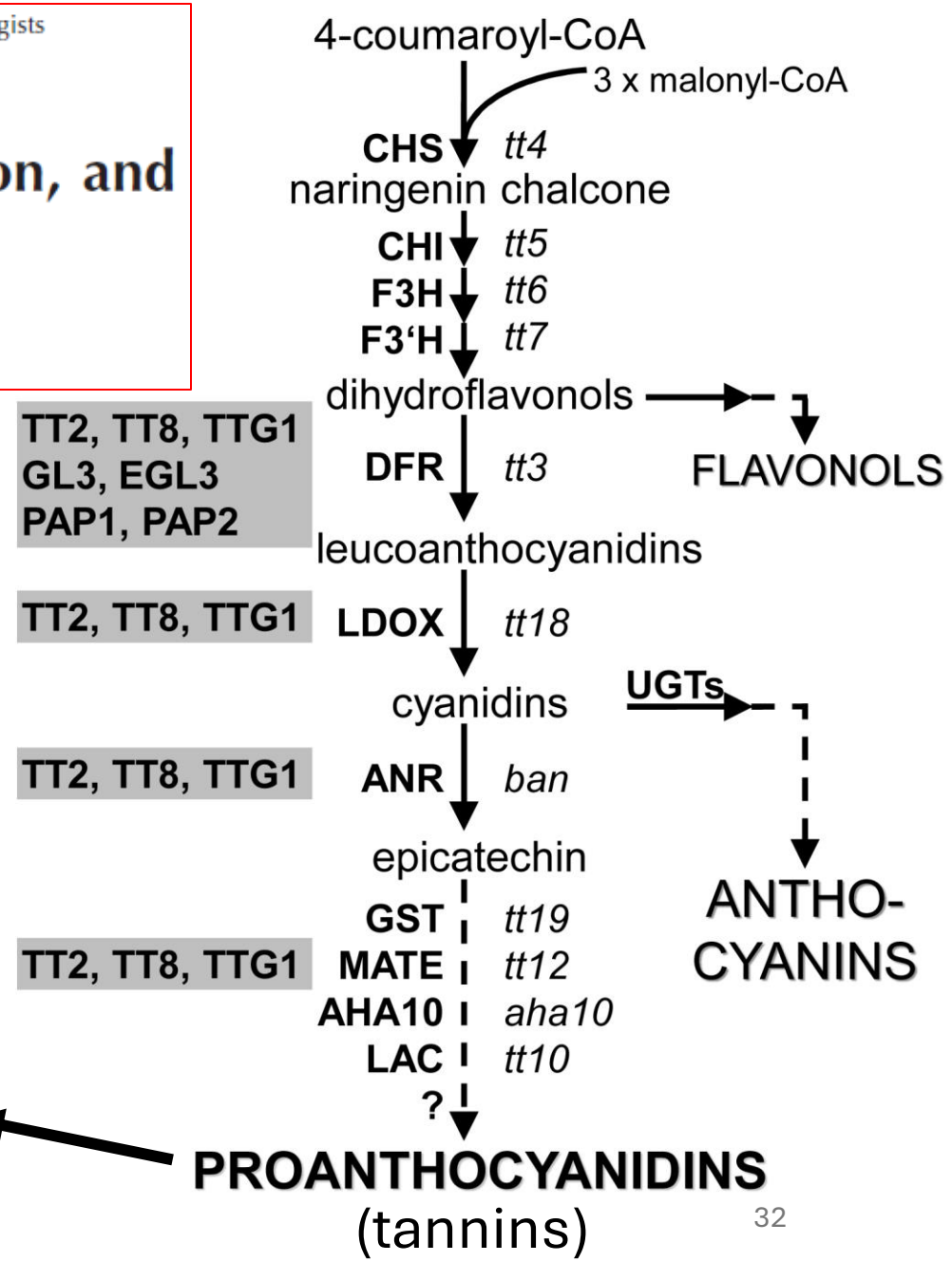

Flavonoid biosynthetic pathway in Arabidopsis (adapted from Shirley, 1998). **The scheme is simplified to show essentially the steps leading to proanthocyanidins, anthocyanins, and flavonols.** Only the mutants corresponding to genes of known function are presented. The mutants in parentheses correspond to regulatory genes, the others to structural genes encoding the enzymes chalcone synthase (CHS), chalcone isomerase (CHI), flavonoid 3-hydroxylase (F3H), flavonoid 39-hydroxylase (F39H), dihydroflavonol reductase (DFR), and a dihydroflavonol reductase-like (DFR-like), as indicated in square brackets. The dashed arrow represents several steps.

Seed coats and transparent testa mutants

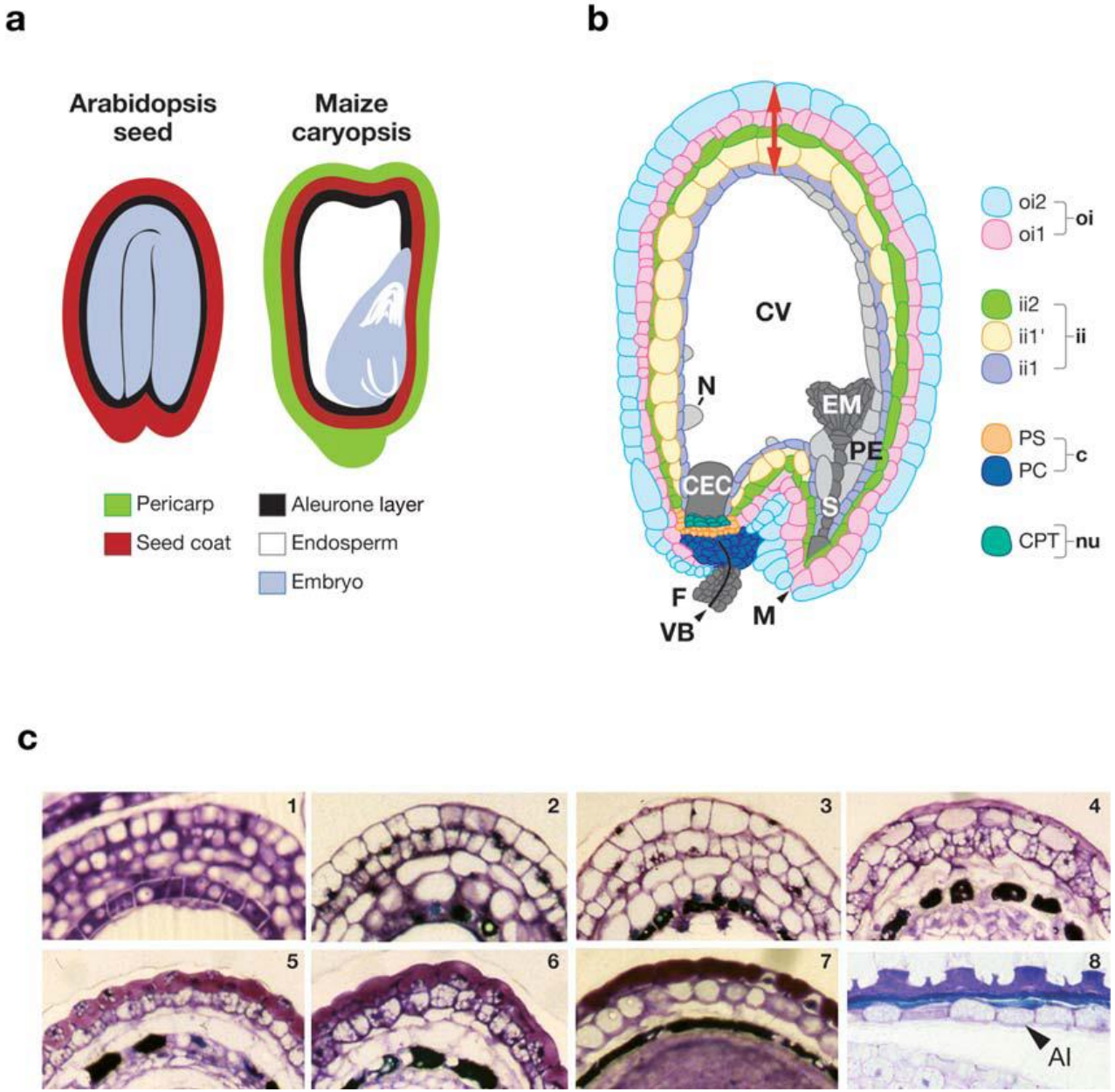

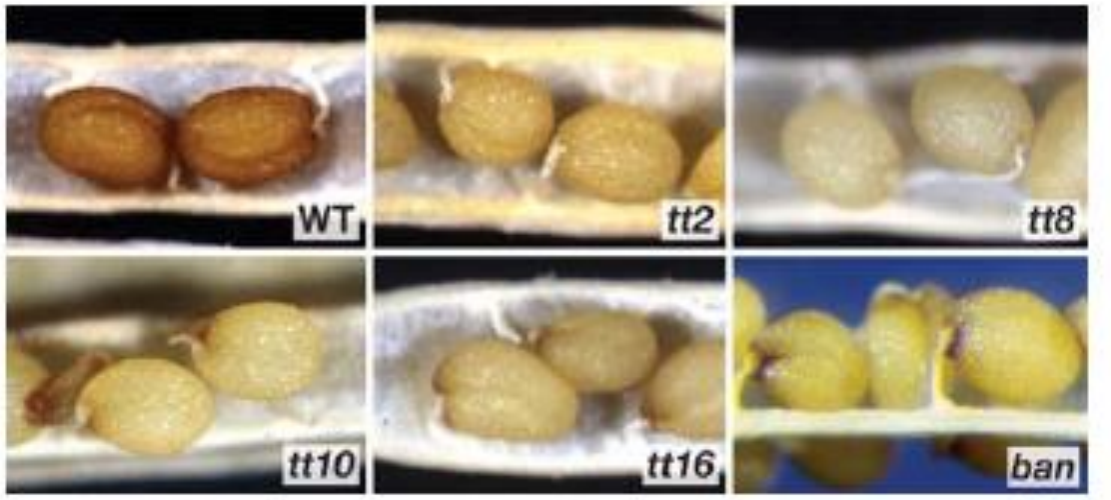

Figure 5

Arabidopsis seed phenotypes in wild-type and some *transparent testa* mutants.

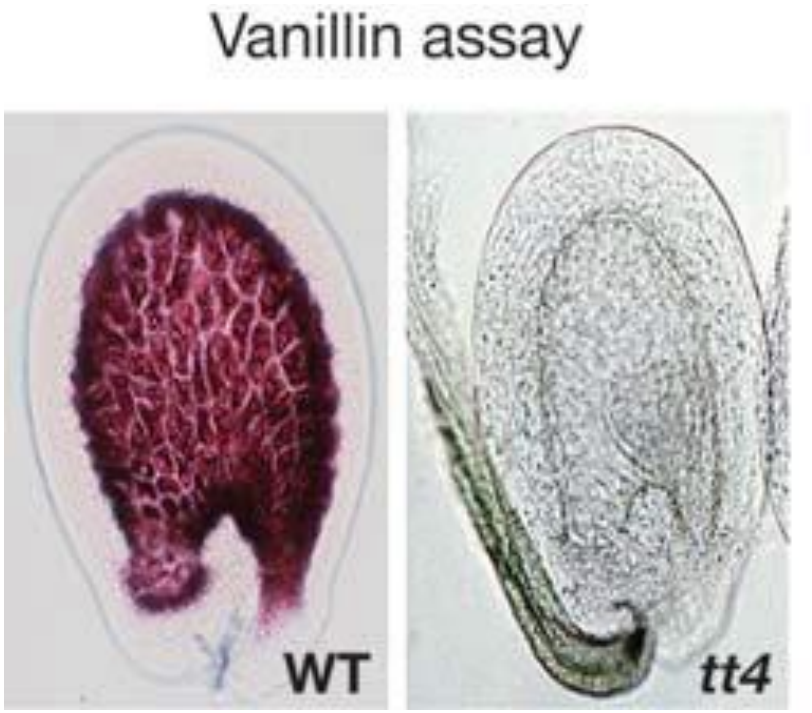

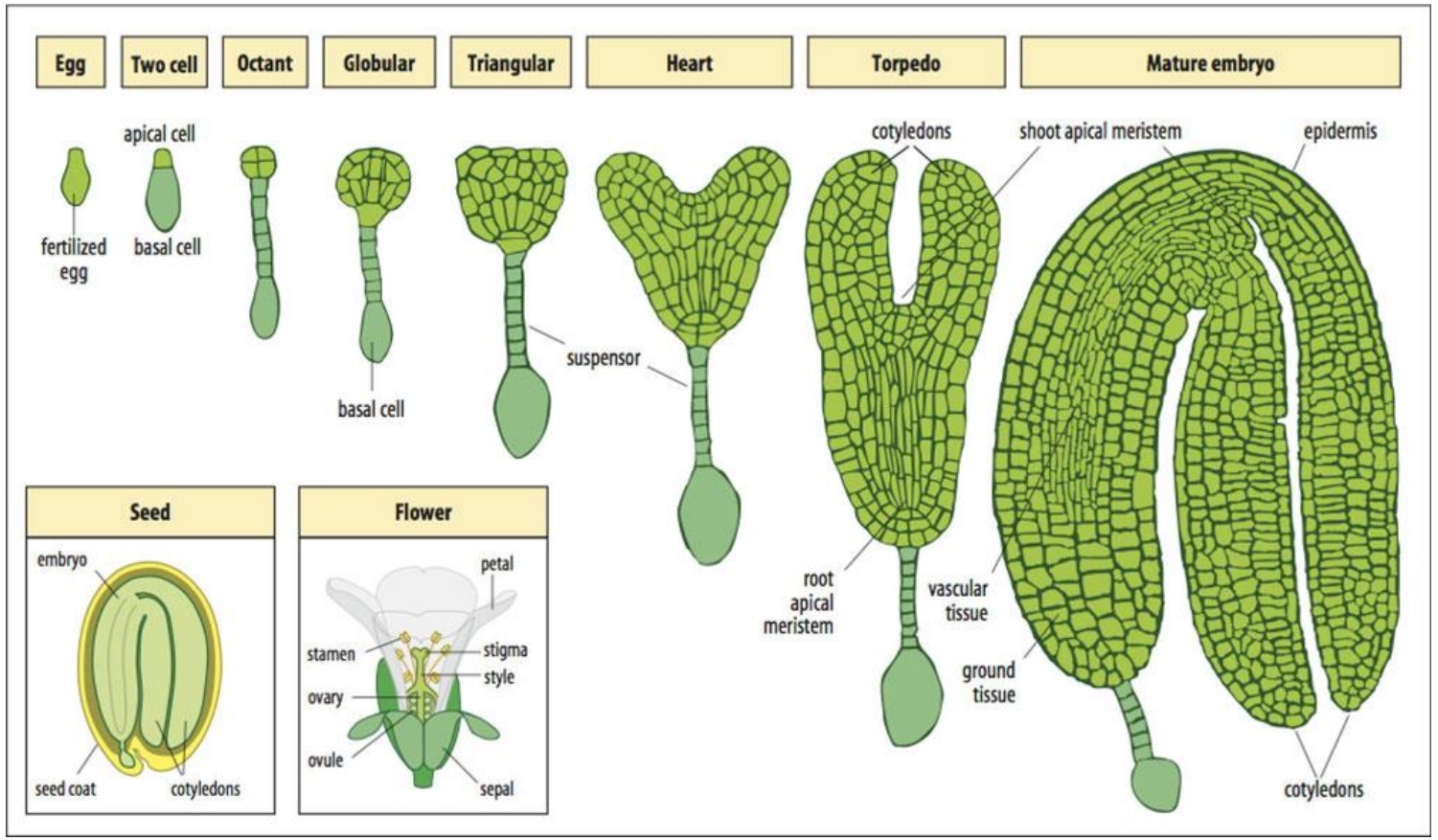

Histochemical detection of seed flavonoids in Arabidopsis. Immature seeds at the late globular-heart stage of embryo development stained as whole mounts. **The vanillin assay is used to detect flavan-3-ols and their proanthocyanidin polymers.**

Characterization of the Arabidopsis seed coat.

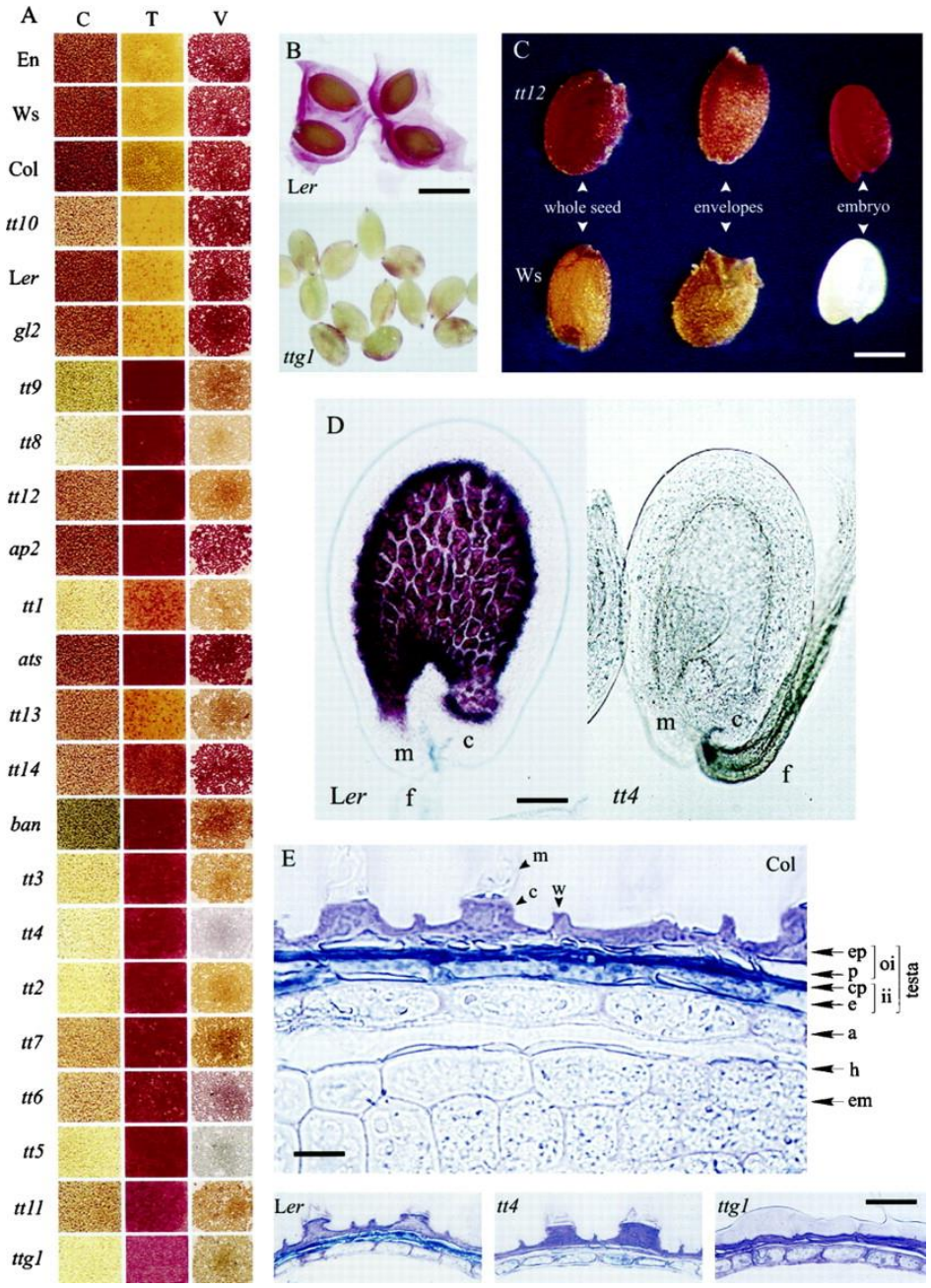

A) The permeability of the testa to tetrazolium salts (T) and the presence of catechins an proanthocyanidins in mature seeds determined by the vanillin assay (V) are compaired with the original color of untreated seeds (C)

Fire frequency is expected to increase with human-induced climate change, especially where precipitation remains the same or is reduced (Stocks et al., 1998).

Leaf size, climate, and energy balance

Wright *et al*. analyzed leaf data for 7670 plant species, along with climatic data, from 682 sites worldwide.

Their findings reveal consistent patterns and explain why earlier predictions from energy balance theory had only limited success.

The authors provide a fully quantitative explanation for the latitudinal gradient in leaf size, with implications for plant ecology and physiology, vegetation modeling, and paleobotany.
Science

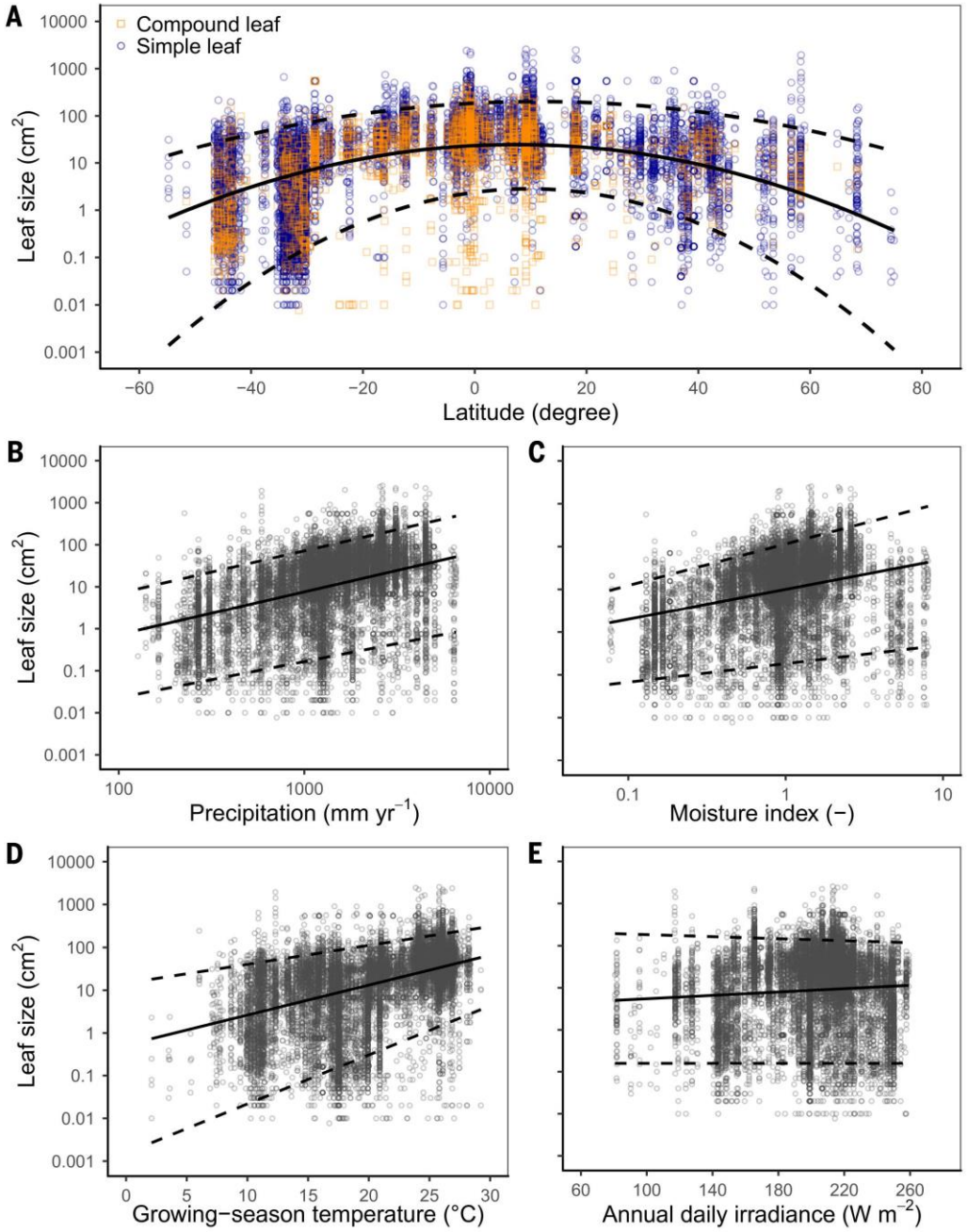

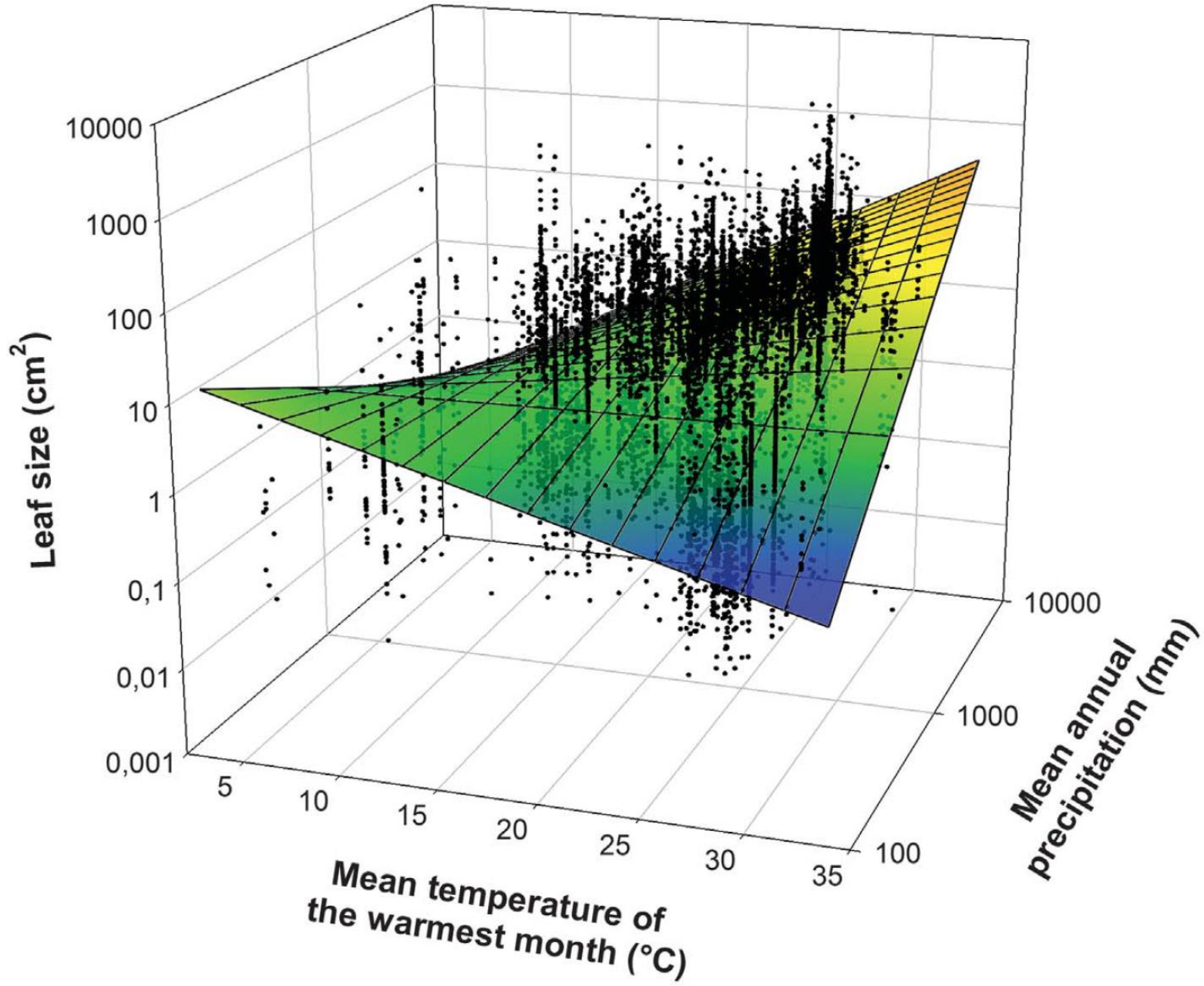

Across the plant kingdom, **leaves vary from less than 1 mm2 to greater than 1 m2 in area**.

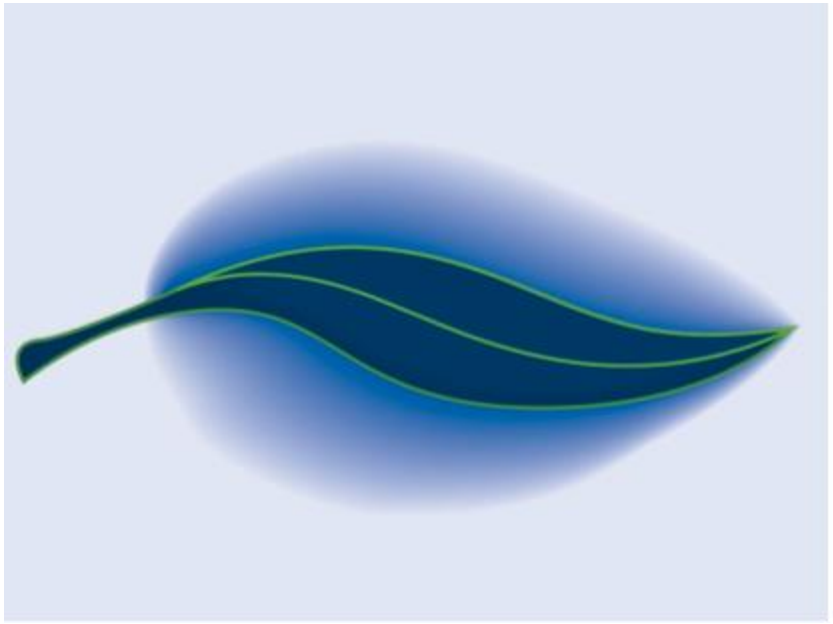

Larger leaves have a **thicker boundary layer** that slows sensible heat exchange with the surrounding air, meaning that—all else equal—they develop **larger leaf-to-air temperature differences than that of smaller leaves**

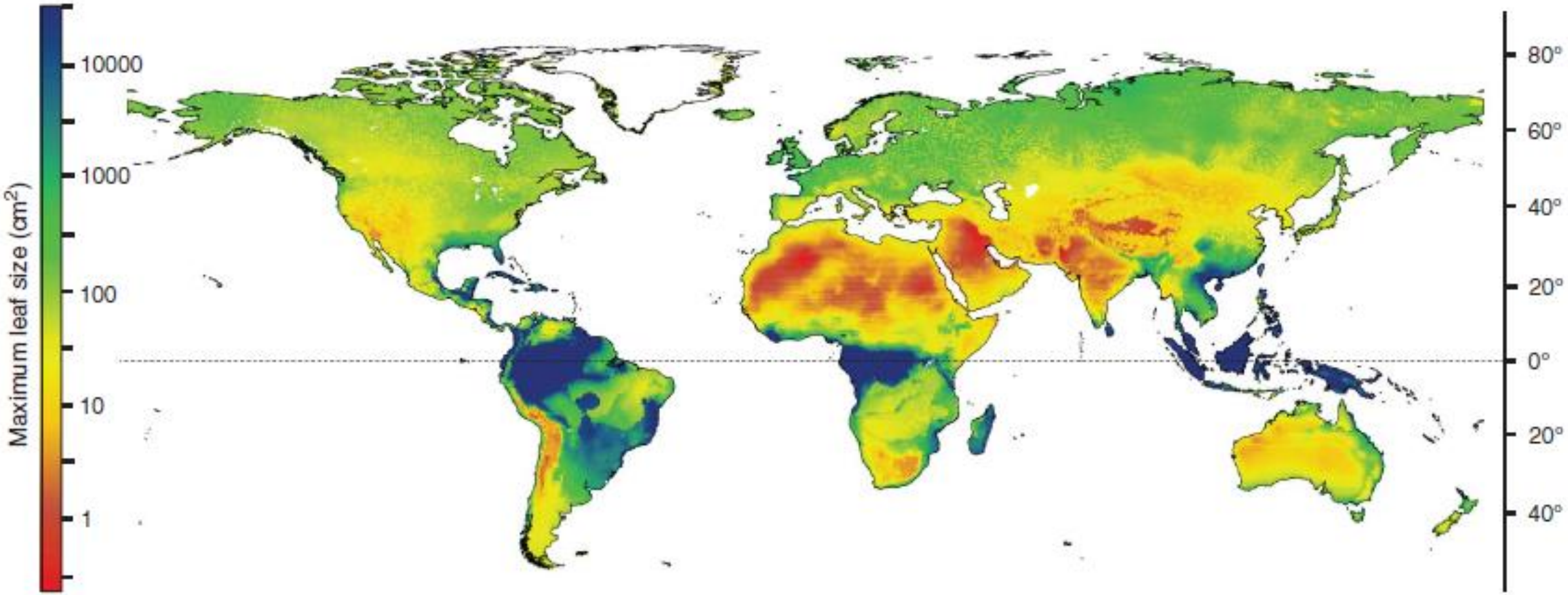
Maximum leaf size (cm²)
10000
1000
100
10
1
80°
60°
40°
20°
0°
20°
40°

What are the selective advantages that favor large leaves under conditions when they are physiologically possible?

This is not well understood, but two prospective explanations seem most promising.

1. First, by deploying a given leaf mass as fewer, larger leaves, the associated **twig costs tend to be lower**, even if within-leaf structural costs are higher
this should lead to a growth advantage

2. Second, the **wider leaf-to-air temperature differences possible for larger leaves may allow them to more quickly heat up to favorable temperatures for photosynthesis during cool mornings**, leading to substantially higher photosynthetic returns.

2. In addition, **under sufficiently hot and high-irradiance conditions**, wider leaf-to-air temperature differences may allow larger leaves to operate at temperatures substantially lower than that of the surrounding air (and more favorable for photosynthesis), provided sufficient soil water is available to support the necessary transpiration.

Fire (heat and smoke) can promote seed germination

Fire stimulates seed release or germination in some plants (fire-ephemerals)

***Banskia* spp, before and after fire**

Some cones and seed pods are fire-serotinous, opening in response to fire

Image sources: pfern, Hesperian, © Kurt Stueber, 2003

- germinate not by the heat of a fire but by the chemicals it produced
- ‘karrik’, which is an Aboriginal term for smoke from the Western Australian Noongar people

Fig. 1. The role of karrikins in revegetation after a fire. A bushfire generates smoke and ash containing karrikins (*upper panel*). After the fire karrikins are present on the soil surface (*middle panel*). After the first rains, the karrikins stimulate germination of the soil seed bank and the growth of new plants, in this case *Anthocercis littorea* (*lower panel*). Top and middle photographs with permission from Vanessa Westcott (Bush Heritage Australia) and bottom photograph from the authors

Karrikins are germination-promoting compounds found in smoke

The butenolide part of the compound is a 5-membered **lactone ring** while the other part of the karrikin compound is a 6-membered **pyran ring**.

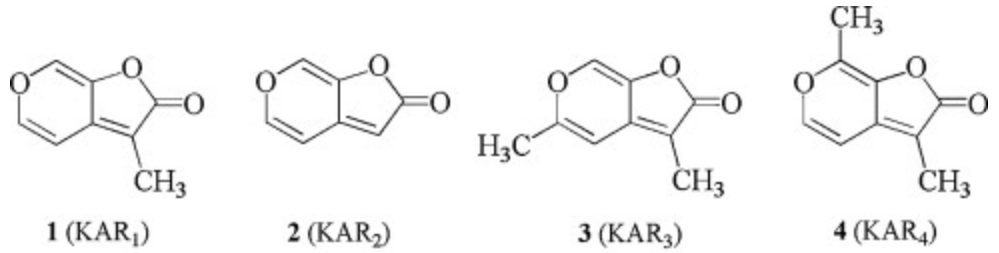

1 (KAR$_1$) **2** (KAR$_2$) **3** (KAR$_3$) **4** (KAR$_4$)

Fire-induced germination lets seedlings become established with less competition from taller plants.

Karrikins are cues from smoke that promote germination.

However, following a fire, there can be increased competition between similarly-sized seedlings….

Reprinted from Chiwocha, S.D.S., Dixon, K.W., Flematti, G.R., Ghisalberti, E.L., Merritt, D.J., Nelson, D.C., Riseborough, J.-A.M., Smith, S.M. and Stevens, J.C. (2009). Karrikins: A new family of plant growth regulators in smoke. Plant Science. 177: 252-256 with permission from Elsevier, and see also Flematti, G. R., et al., (2004). A compound from smoke that promotes seed germination. Science 305: 977.

Partial structural similarity between the karrikin family of plant growth regulators and strigolactones.

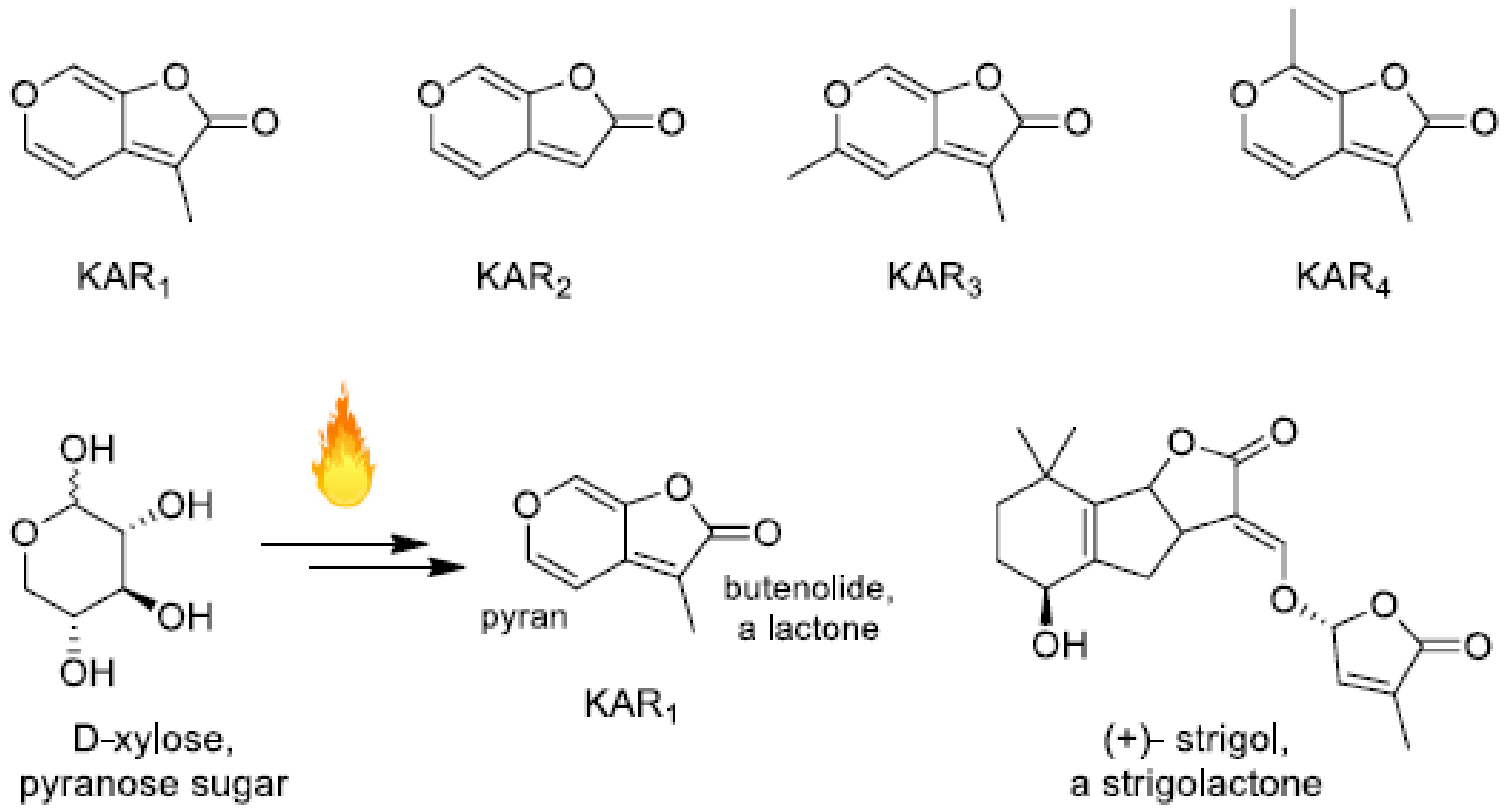

Fig. 2. The karrikin family. The first karrikin discovered was KAR_1, also known as karrikinolide. Since karrikins can be produced by burning sugars such as xylose, the pyran ring of karrikins is probably derived from such pyranose sugars. Both karrikins and strigolactone hormones such as strigol have a butenolide ring

David C. Nelson et al. Plant Physiol. 2009;149:863-873

Strigolactone biosynthesis is related to carotenoid catabolism

a

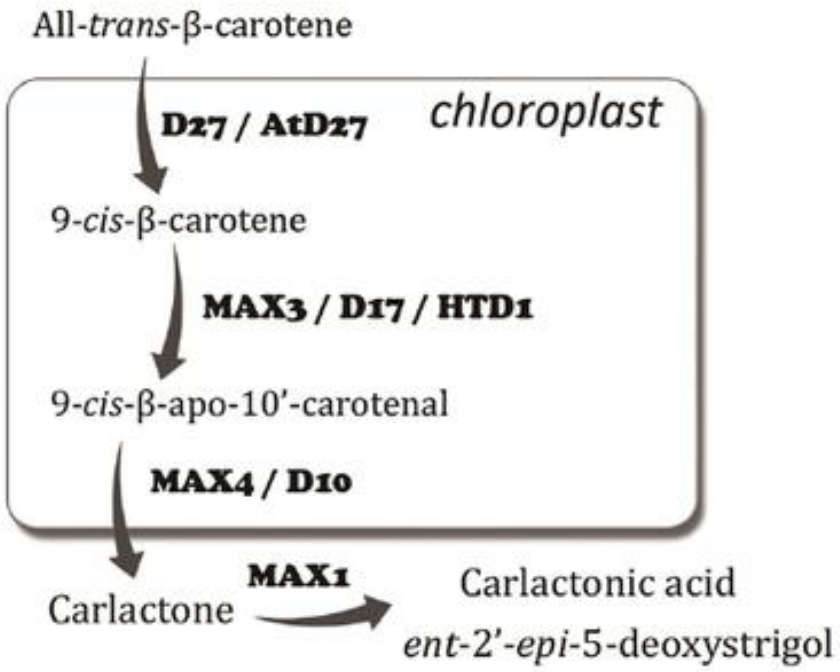

b

Enzyme	*Arabidopsis* gene	Rice gene
D27	*AtD27* (At1g03055)	*D27* (Os11g0587000)
CCD7	*MAX3* (At2g42620)	*D17/HTD1* (Os04g0550600)
CCD8	*MAX4* (At4g32810)	*D10* (Os01g0746400)
MAX1	*MAX1* (At2g26170)	*OsMAX1* (Os1g0700900; Os01g0701500 Os01g0701400; Os02g0221900 Os06g0565100)

Also other smoke molecules can stimulate seed germination

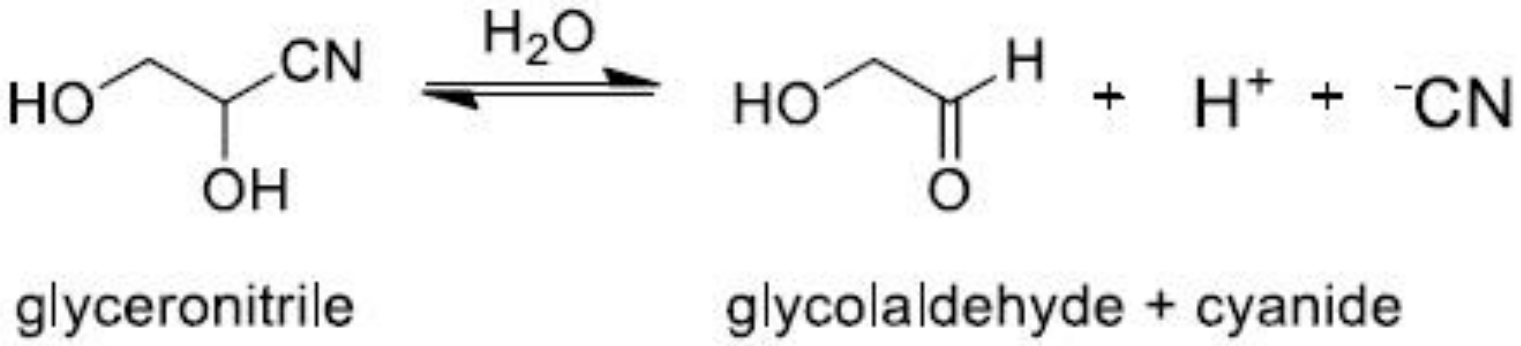

Fig. 4. Germination of *Arabidopsis* seeds and growth of seedlings in response to karrikin. *Arabidopsis thaliana* seeds with primary dormancy incubated for seven days on water-agar without karrikin (KAR) germinate very poorly whereas those with KAR germinate readily (top row). Seedlings germinated on nutrient medium and grown in low light for seven days without KAR have long hypocotyls whereas those with KAR have short hypocotyls and larger cotyledons (bottom row). Images from the author's laboratory

Karrikins are involved also in other physilogical responses

karrikins are unstable at very high temperatures.

It is likely, therefore, that they are produced in **the less-intense parts of wildfires, vaporise, and collect in the smoke and condensation** and become bound to soil particles in the same way that cooled smoke can be deposited onto seeds to stimulate their germination.

Karrikins may be 'carried' in smoke by a process of steam distillation but are **not carried for long distances** in smoke, and largely remain close to the source of the fire

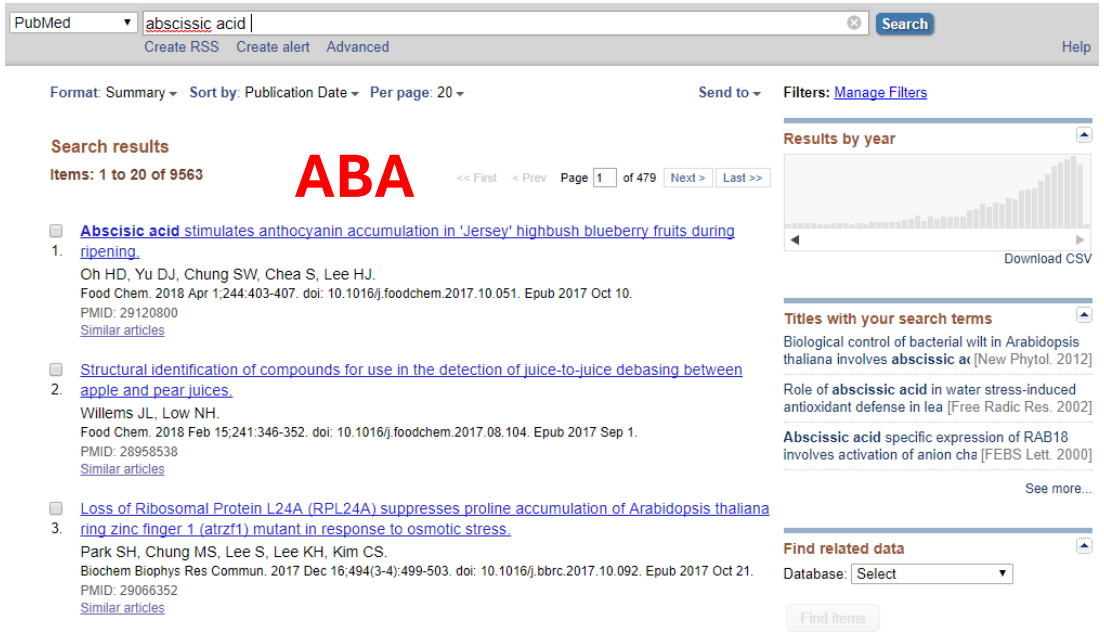

Their production from polysaccharides and sugars explains the pyran ring of karrikins

The smoke from cigarettes stimulates seed germination, probably due to the presence of karrikins.

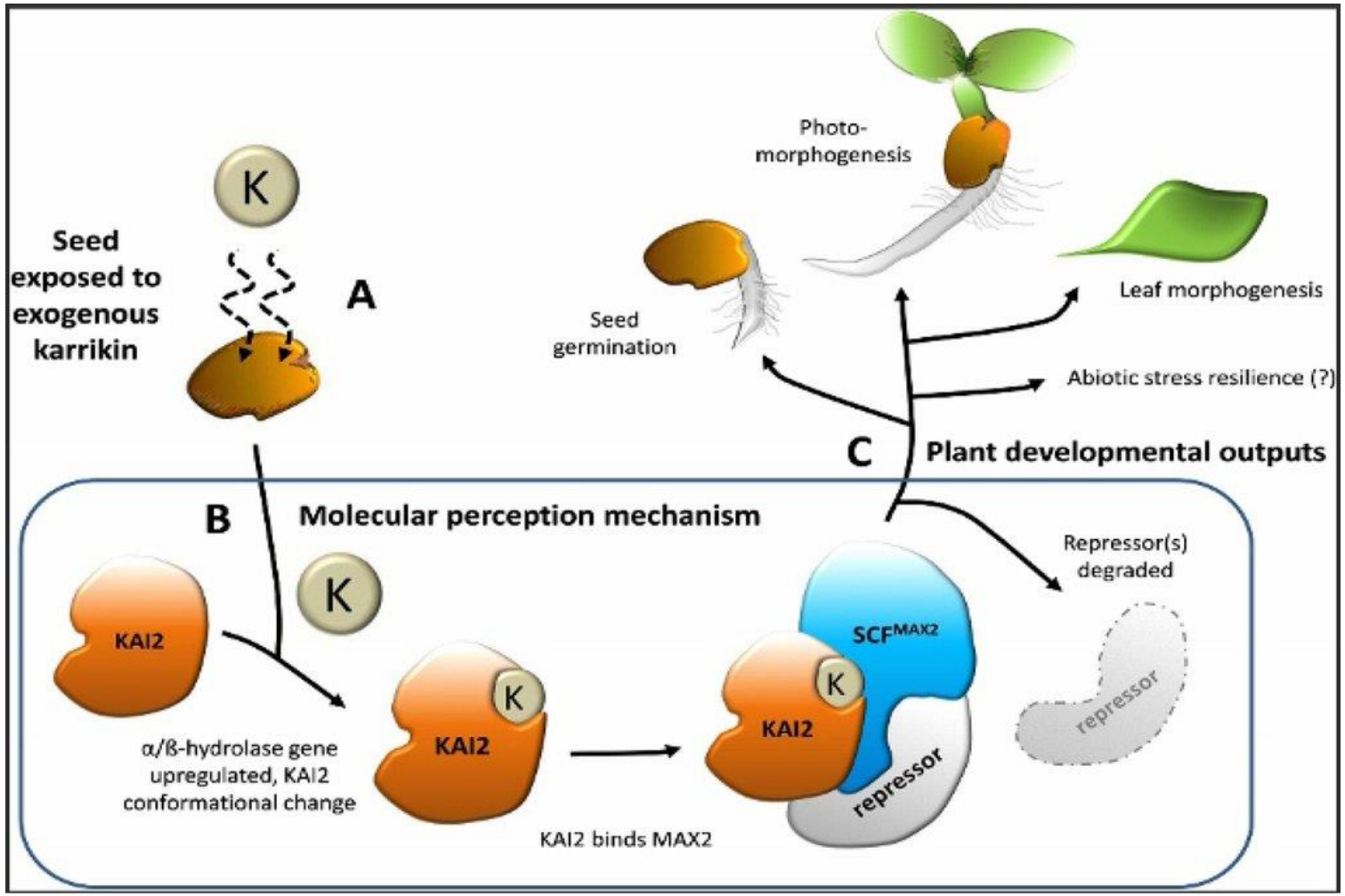
K
Seed exposed to exogenous karrikin
A
Photo-morphogenesis
Seed germination
Leaf morphogenesis
Abiotic stress resilience (?)
C
Plant developmental outputs
B
Molecular perception mechanism
K
KAI2
α/ß-hydrolase gene upregulated, KAI2 conformational change
KAI2 binds MAX2
SCFMAX2
repressor
Repressor(s) degraded
repressor

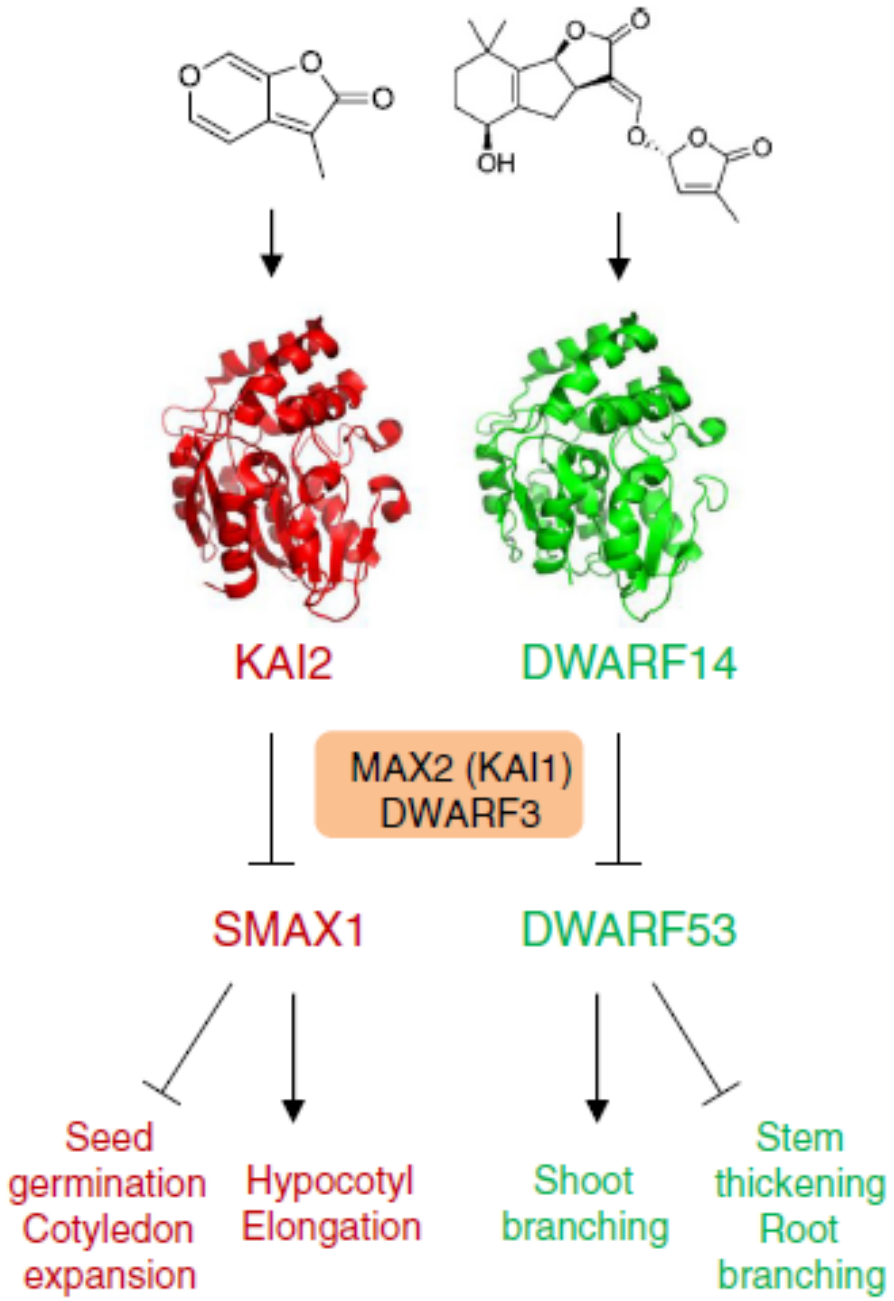

KARRIKIN-INSENSITIVE 2 is structurally similar to the receptor of strigolactone DWARF14

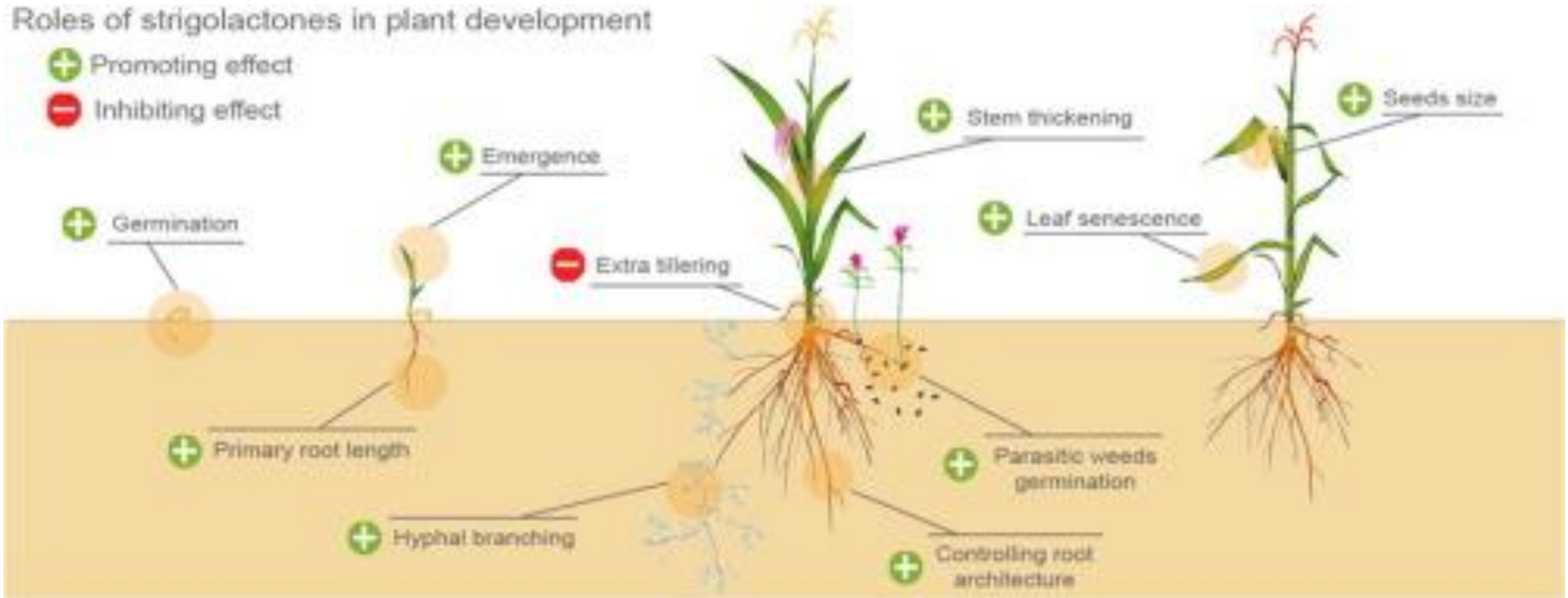
Roles of strigolactones in plant development
Promoting effect
Inhibiting effect
Germination
Emergence
Primary root length
Extra tillering
Stem thickening
Leaf senescence
Seeds size
Parasitic weeds germination
Hyphal branching
Controlling root architecture

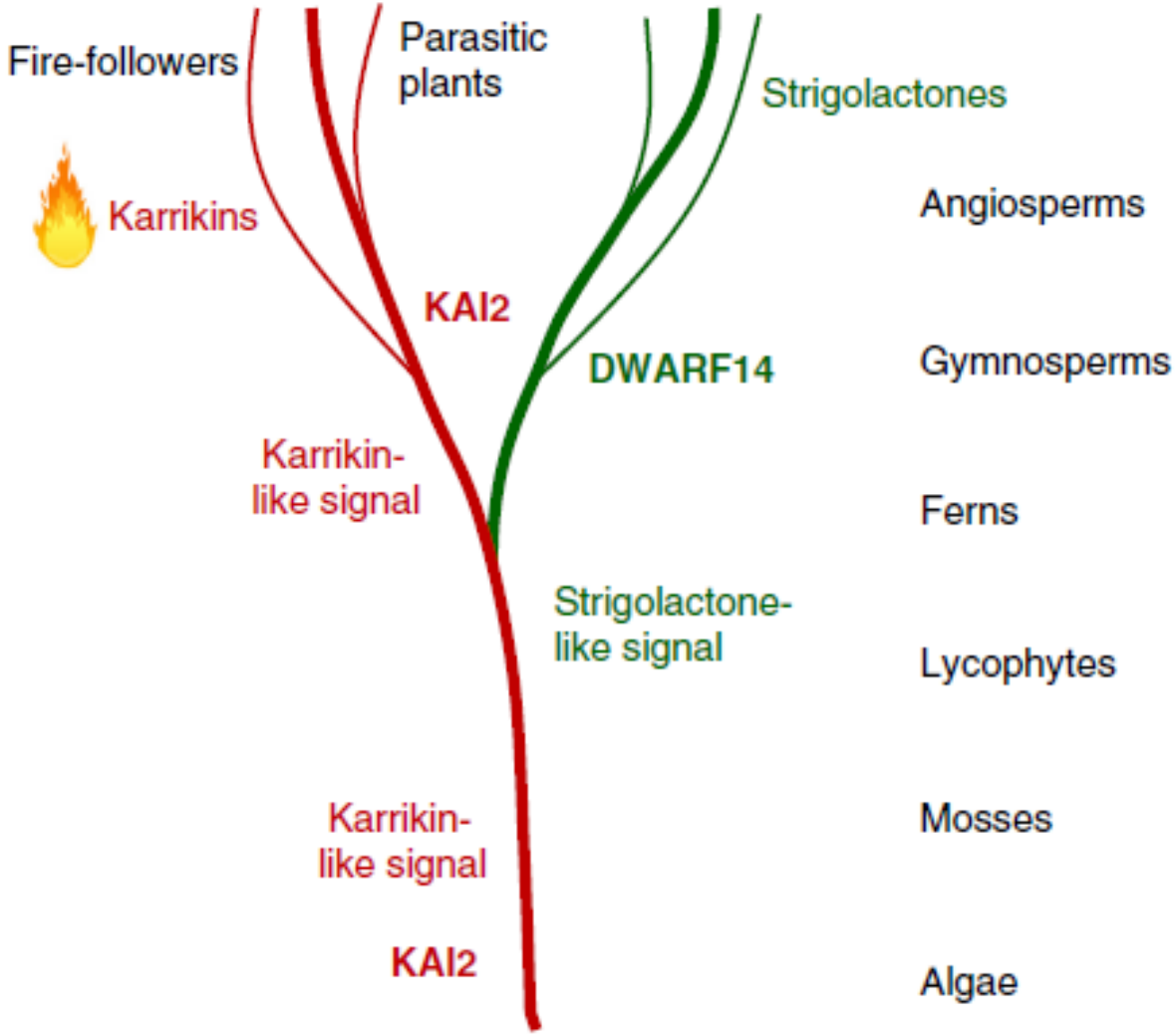

Fig. 7. Possible evolution of the karrikin response system in plants. The *KAI2* gene can be traced back to single-celled algae. Gene duplication before the evolution of seed plants leading to *DWARF14* genes probably provided the opportunity for functional specialisation of *KAI2*-type genes, including roles in the response to karrikins and the response of parasitic plants to host-derived strigolactones. The origin of strigolactones is unclear since mosses are reported to produce them. Karrikin-like signals distinct from strigolactones probably have an ancient origin

New Phytologist

Research

Fire-adapted traits of *Pinus* arose in the fiery Cretaceous

Tianhua He[1,2,3], Juli G. Pausas[4], Claire M. Belcher[5], Dylan W. Schwilk[6] and Byron B. Lamont[2,7]

- Fire-protective thick bark originated in Pinus c. 126 Ma in association with low-intensity surface fires. More intense crown fires emerged c. 89 Ma coincident with thicker bark and branch shedding, or serotiny with branch retention as an alternative strategy.

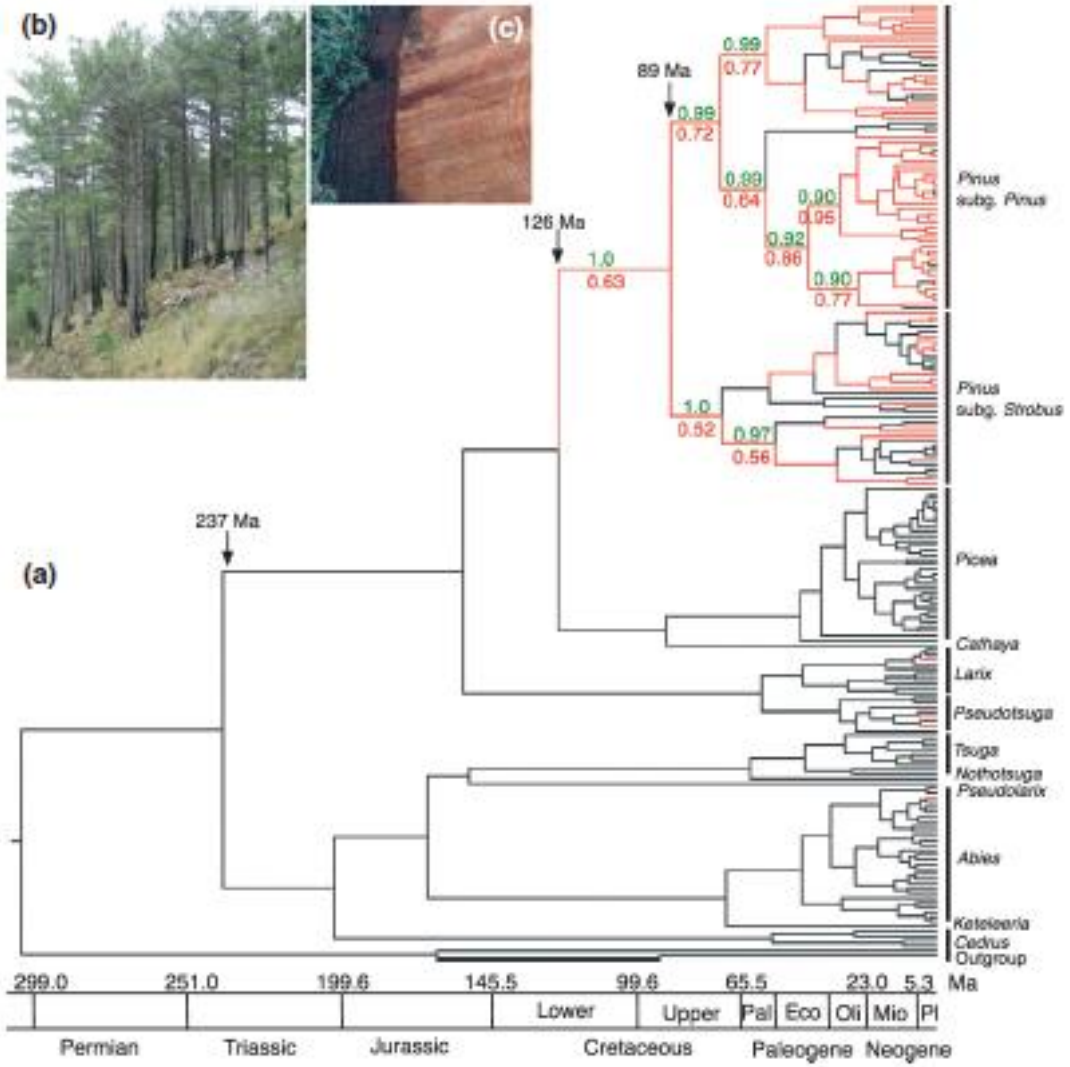

These innovations appeared at the same time as the Earth's paleoatmosphere experienced elevated oxygen levels that led to high burn probabilities during the mid-Cretaceous.

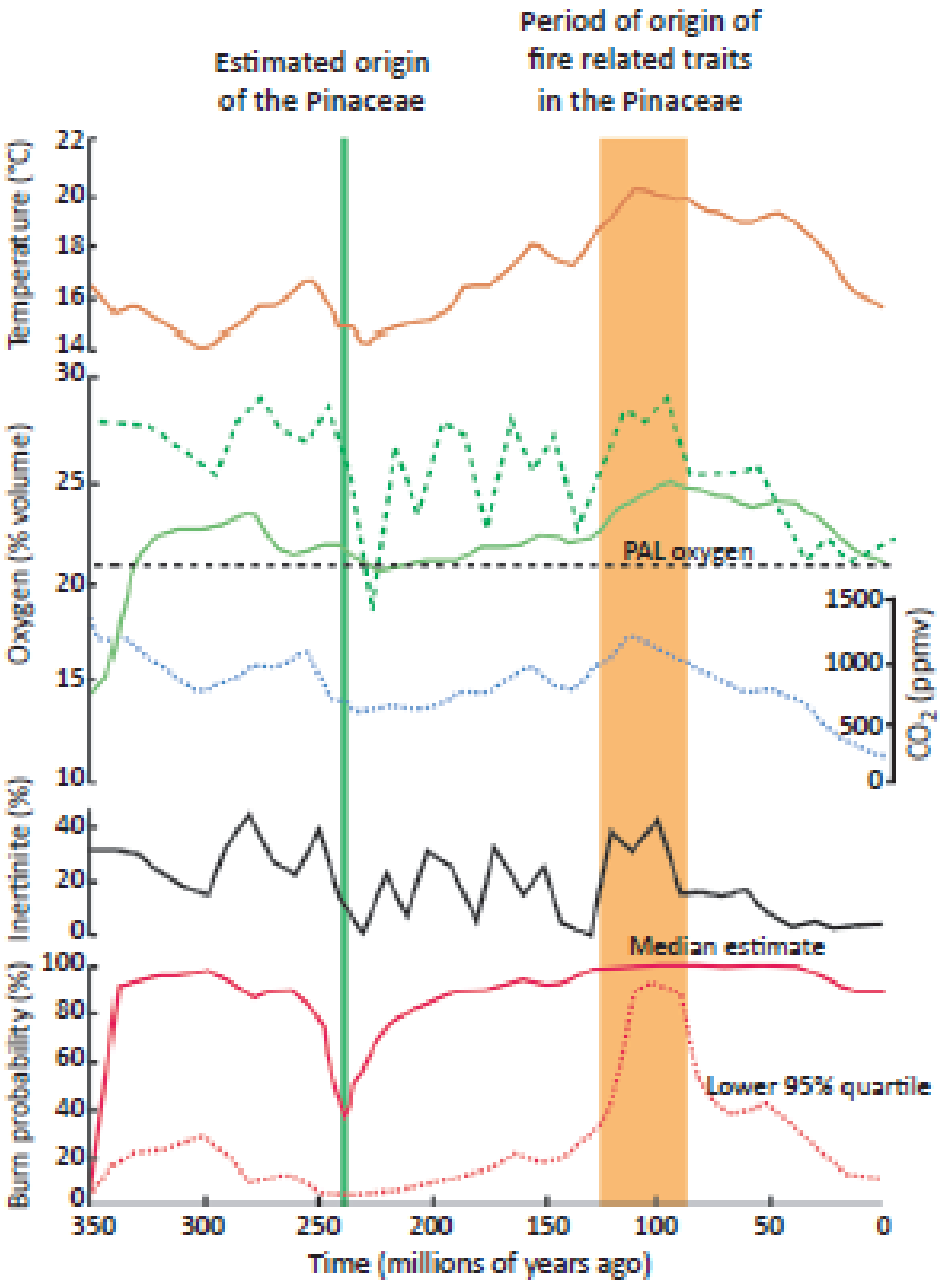

Karrikins enhance germination of Arabidopsis.

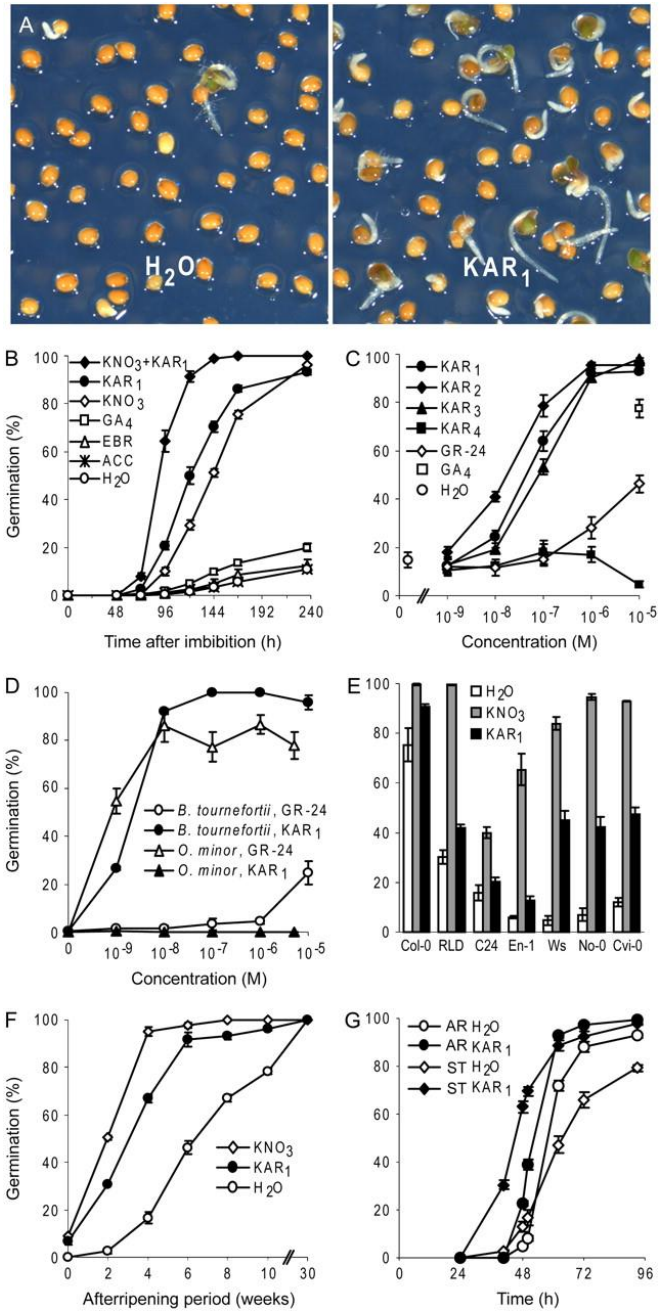

Karrikins enhance germination of Arabidopsis. **A, PD L*er* seeds** after 5 d of imbibition on water (left) or 1 μm KAR_1 (right). B, Germination of PD L*er* seeds imbibed on 10 mm KNO_3, 1 μm KAR_1, GA_4, or EBR, or 10 μm ACC. C, Germination of PD L*er* seeds after 7 d of imbibition on 1 nm to 10 μm KAR_1, KAR_2, KAR_3, or KAR_4, GR-24, or GA_4. D, Germination of *B. tournefortii* and the parasitic weed *O. minor* in the presence of GR-24 or KAR_1. **E, Germination of PD Arabidopsis ecotypes** after 7 d of imbibition (except Cvi-0, which is shown at 14 d). Time courses of germination are shown in Supplemental Figure S1. F, Germination of progressively AR PD L*er* seeds after 4 d of imbibition. G, Germination of PD L*er* stratified (ST) for 3 d in the dark at 4°C or 10-month AR L*er* seeds (AR) ± 1 μm KAR_1. The *x* axis indicates the time after transfer to continuous light at 20°C or the time of imbibition.

Responses of phytohormone mutants to KAR1.

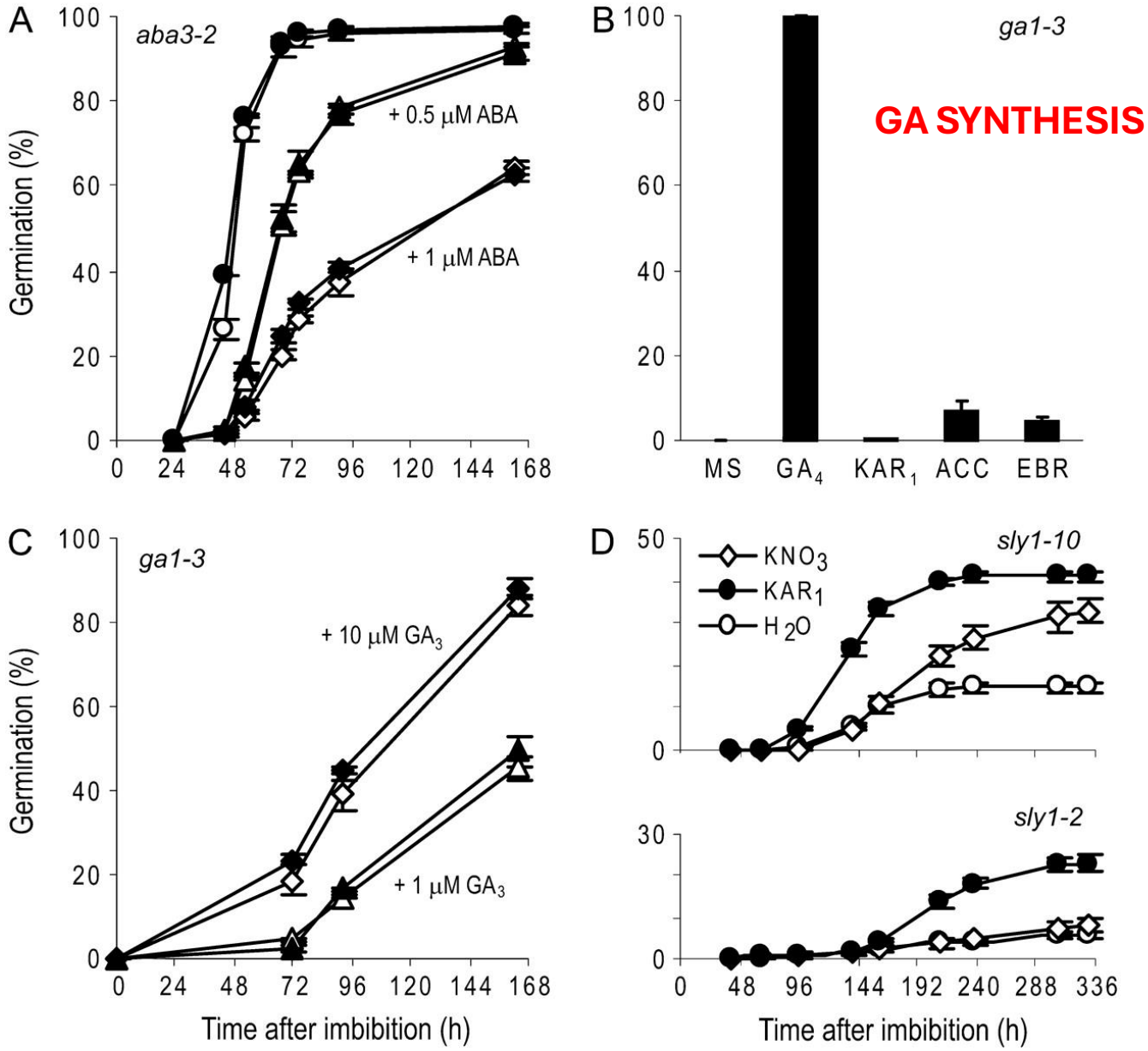

A, Germination of *aba3-2* on ABA with (black symbols) or without (white symbols) 1 μm KAR_1. B, Germination of *ga1-3* after a 3-d dark stratification at 4°C followed by 10 d in continuous light at 20°C. The medium was 0.5× Murashige and Skoog salts (MS; contains nitrates) with 10 μm GA_4, 1 μm KAR_1, 10 μm ACC, or 1 μm EBR. C, Germination of *ga1-3* in the presence of 1 or 10 μm GA_3 ± 1 μm KAR_1. D, Germination of *sly1-10* and *sly1-2* alleles.

David C. Nelson et al. Plant Physiol. 2009;149:863-873

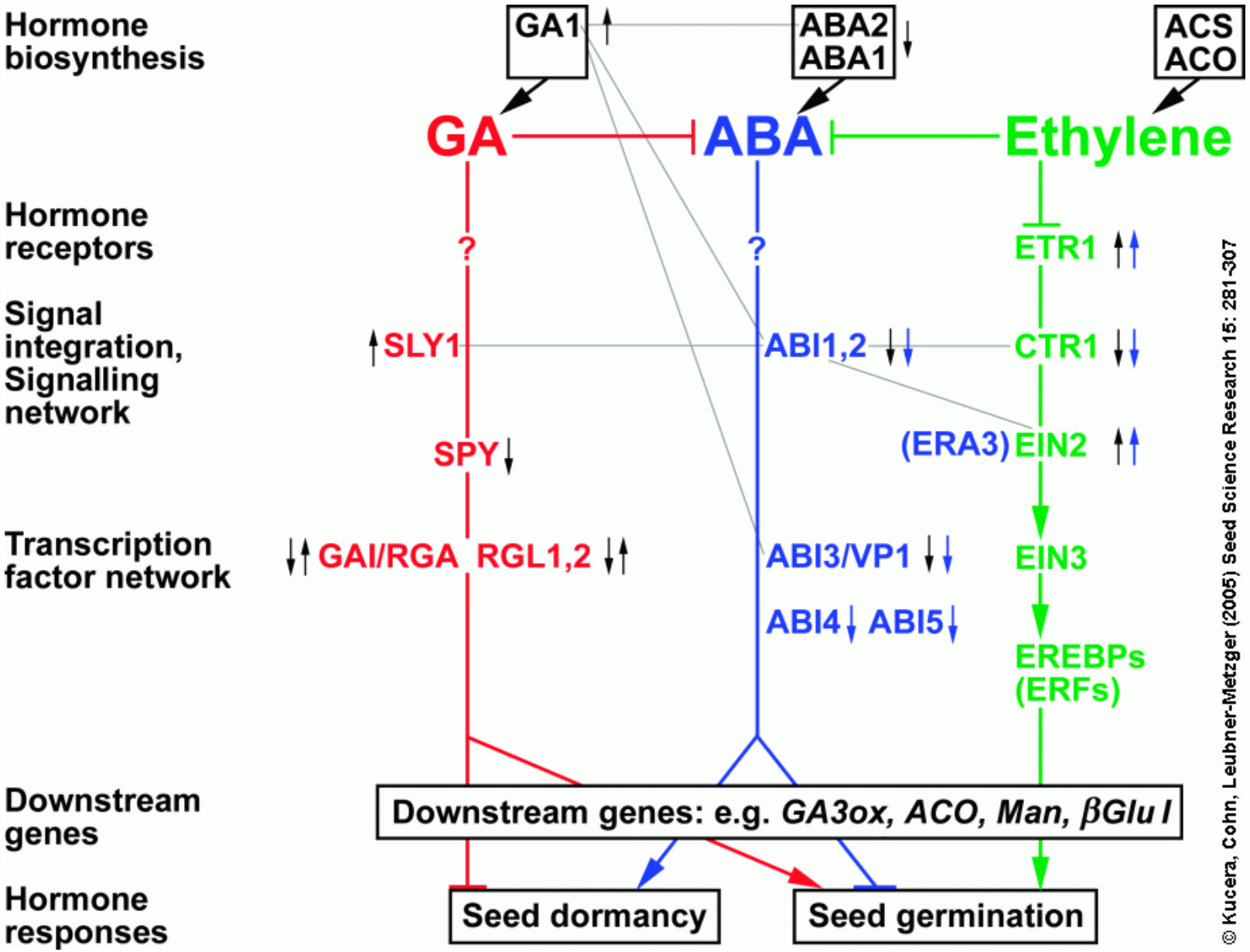
Hormone biosynthesis
Hormone receptors
Signal integration, Signalling network
Transcription factor network
Downstream genes
Hormone responses
GA1
ABA2
ABA1
ACS
ACO
GA
ABA
Ethylene
?
?
ETR1
SLY1
ABI1,2
CTR1
SPY
(ERA3)
EIN2
GAI/RGA
RGL1,2
ABI3/VP1
EIN3
ABI4
ABI5
EREBPs
(ERFs)
Downstream genes: e.g. GA3ox, ACO, Man, βGlu I
Seed dormancy
Seed germination
© Kucera, Cohn, Leubner-Metzger (2005) Seed Science Research 15: 281-307

Karrikins induce GA 3-oxidase and CP1 transcripts.

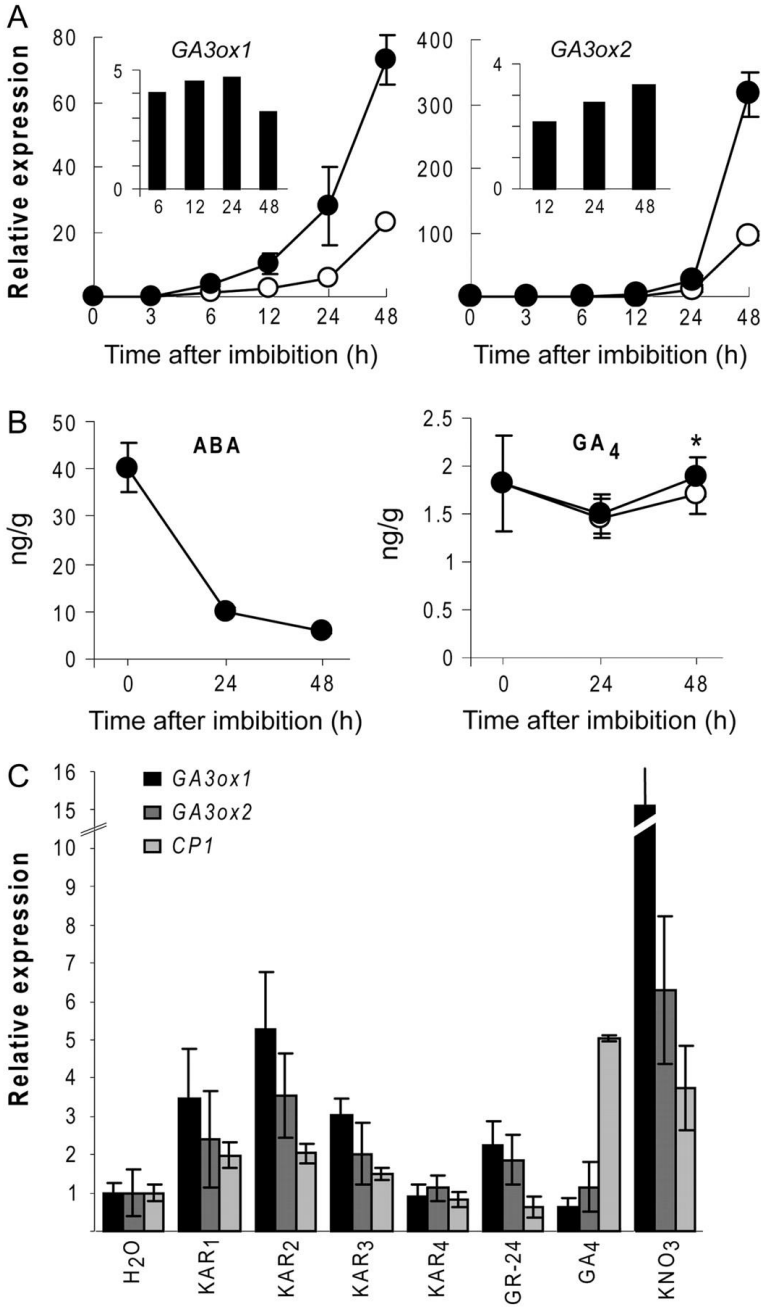

David C. Nelson et al. Plant Physiol. 2009;149:863-873

KAR1 requires light to induce germination and does not enhance GA perception.

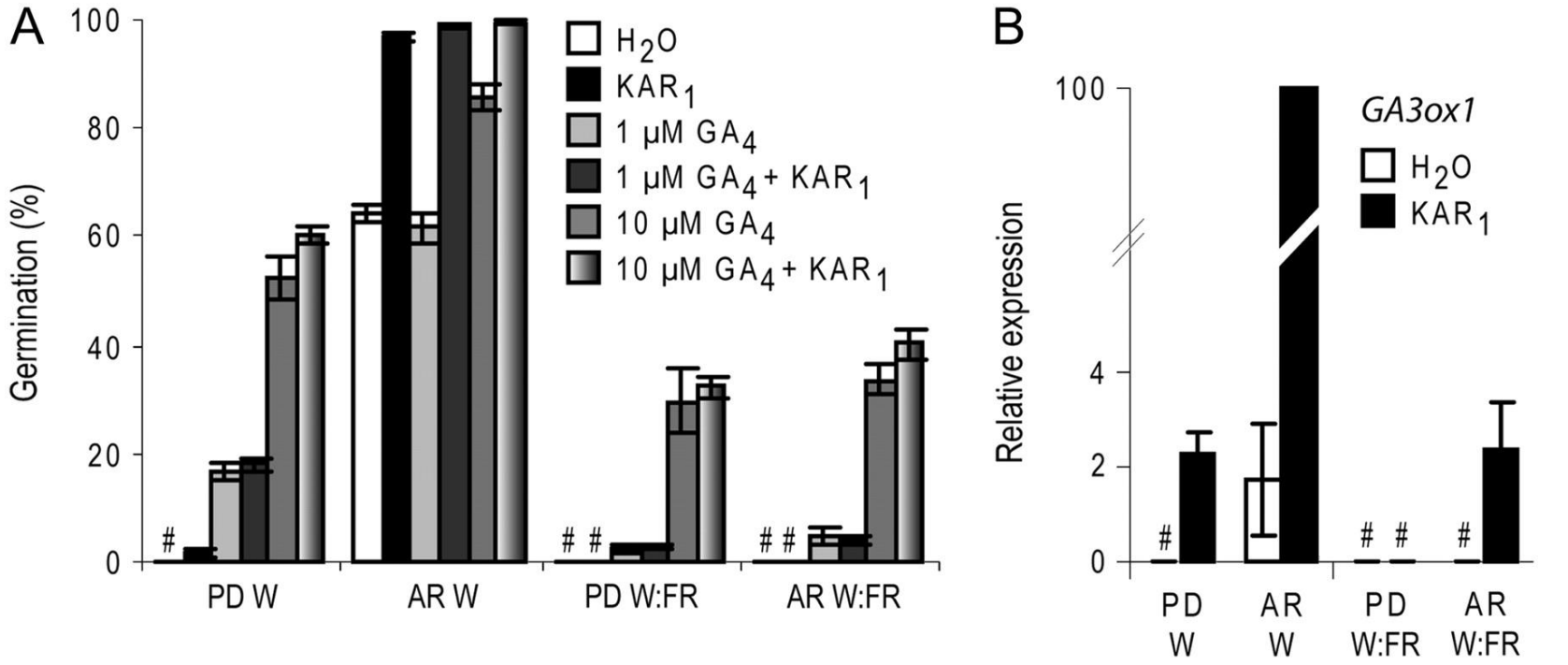

David C. Nelson et al. Plant Physiol. 2009;149:863-873

How long do karrikins remain in the soil?

Measurements of karrikins in soil are technically very challenging but seed-germination bioassays can be used to detect activity, one study suggesting that active compound(s) can persist in the soil for over seven years after a fire [7]. Karrikins are unstable in ultraviolet light [6] so they might be expected to decay rapidly in natural sunlight; however, smoke contains many aromatic compounds that can absorb ultraviolet light and could protect karrikins by acting as organic 'sunscreens'. On the other hand, **karrikins can be washed away by rain** and elute through sandy soils relatively quickly, so their concentration will steadily decline.

What type of plants respond to karrikins?

Seeds from **many different families** of flowering plants and conifers representing many plant life forms (trees, shrubs, herbs, annuals) will respond to karrikins, and many more respond to smoke, implying that the karrikin response is **widespread** and may have evolved independently in different groups [1]. Plants with smoke-responsive seed are found in both fire-prone and non-fire-prone environments. Most are dicotyledonous plants but many grasses also respond to smoke. **Surprisingly, not only fire-followers respond but also many weedy species, including agricultural weeds**